

1     **Systematic prioritization of candidate genes in disease loci identifies *TRAFD1* as a**  
2                     **master regulator of IFN $\gamma$  signalling in celiac disease**

3     Adriaan van der Graaf<sup>1#</sup>, Maria Zorro<sup>1#</sup>, Annique Claringbould<sup>1</sup>, Urmo Vosa<sup>1,2</sup>, Raul Aguirre-  
4     Gamboa<sup>1</sup>, Chan Li<sup>1,3</sup>, Joram Mooiweer<sup>1</sup>, Isis Ricano-Ponce<sup>1</sup>, Zuzanna Borek<sup>4,5</sup>, Frits  
5     Koning<sup>6</sup>, Yvonne Kooy-Winkelaar<sup>6</sup>, Ludvig Sollid<sup>3</sup>, Shuo-Wang Qiao<sup>3</sup>, BIOS consortium,  
6     Vinod Kumar<sup>1,7</sup>, Yang Li<sup>1,7,8</sup>, Lude Franke<sup>1</sup>, Sebo Withoff<sup>1</sup>, Cisca Wijmenga<sup>1,3</sup>, Serena  
7     Sanna<sup>1,9#\*</sup>, Iris Jonkers<sup>1,3#\*</sup>.

8     **Affiliations**

9     <sup>1</sup> Department of Genetics, University Medical Center Groningen, University of Groningen,  
10    Groningen, the Netherlands

11    <sup>2</sup> Estonian Genome Center, Institute of Genomics, University of Tartu, Tartu, Estonia

12    <sup>3</sup> Department of Immunology, K.G. Jebsen Coeliac Disease Research Centre, University of  
13    Oslo, Oslo, Norway

14    <sup>4</sup> Deutsches Rheumaforschungszentrum Berlin (DRFZ), An Institute of the Leibniz  
15    Association, Berlin, Germany

16    <sup>5</sup> Charité – Universitätsmedizin Berlin, corporate member of Freie Universität Berlin,  
17    Humboldt-Universität zu Berlin, and Berlin Institute of Health, Department of  
18    Gastroenterology, Infectious Diseases and Rheumatology, Berlin, Germany

19    <sup>6</sup> Department of Immunohematology and Blood Transfusion, Leiden University Medical  
20    Center, Leiden, the Netherlands

21    <sup>7</sup> Department of Internal Medicine and Radboud Center for Infectious Diseases (RCI),  
22    Radboud University Medical Center, Nijmegen, the Netherlands

23    <sup>8</sup> Department of Computational Biology for Individualised Infection Medicine, Centre for  
24    Individualised Infection Medicine, Helmholtz Centre for Infection Research, Hannover  
25    Medical School, Hannover, Germany

26    <sup>9</sup> Istituto di Ricerca Genetica e Biomedica (IRGB) del Consiglio Nazionale delle Ricerche  
27    (CNR), Monserrato, Italy

28

29    # These authors contributed equally

30    \*Corresponding Authors

31

32 **Abstract**

33

34 **Background:** Celiac disease (CeD) is a complex T cell-mediated enteropathy induced by  
35 gluten. Although genome-wide association studies have identified numerous genomic  
36 regions associated with CeD, it is difficult to accurately pinpoint which genes in these loci are  
37 most likely to cause CeD.

38 **Results:** We used four different *in silico* approaches – Mendelian Randomization inverse  
39 variance weighting, COLOC, LD overlap and DEPICT – to integrate information gathered  
40 from a large transcriptomics dataset. This identified 118 prioritized genes across 50 CeD-  
41 associated regions. Co-expression and pathway analysis of these genes indicated an  
42 association with adaptive and innate cytokine signalling and T cell activation pathways. 51 of  
43 these genes are targets of known drug compounds and likely druggable genes, suggesting  
44 that our methods can be used to pinpoint potential therapeutic targets. In addition, we  
45 detected 172 gene-combinations that were affected by our CeD-prioritized genes in *trans*.  
46 Notably, 41 of these *trans*-mediated genes appear to be under control of one master  
47 regulator, *TRAFD1*, and were found to be involved in IFN $\gamma$  signalling and MHC I antigen  
48 processing/presentation. Finally, we performed *in vitro* experiments that validated the role of  
49 *TRAFD1* as an immune regulator acting in *trans*.

50 **Conclusions:** Our strategy has confirmed the role of adaptive immunity in CeD and  
51 revealed a genetic link between CeD and the IFN $\gamma$  signalling and MHC I antigen processing  
52 pathways, both major players of immune activation and CeD pathogenesis.

53

54

55 **Key words:** Celiac disease, gene prioritization, expression quantitative trait loci (eQTL)

56

57

## 58 **Glossary**

59 Underlined words are definitions that have been explained in the preceding lines.

60

61 **eQTL** – expression quantitative trait locus, a location on the genome that is statistically  
62 associated to changes in gene expression.

63 **cis-eQTL** – an eQTL located in the same locus of the gene that is being interrogated (within  
64 1.5Mb from gene transcript start or end).

65 **trans-eQTL** – an eQTL that is not physically close to the gene that is being interrogated  
66 (>1.5Mb from transcript start/end or on a different chromosome).

67 **cis-eQTL gene** – a gene that is associated with a change in expression as a consequence  
68 of a cis-eQTL.

69 **trans-eQTL gene** – a gene that is associated with a change in expression as a  
70 consequence of a trans-eQTL.

71 **CeD** – celiac disease

72 **CeD-associated region** – a genomic region that is associated to CeD based on results from  
73 genome-wide association studies on CeD.

74 **Prioritized gene** – a gene prioritized as being potentially causal for CeD according to the  
75 four statistical methods depicted in Figure 1A-B. In this study, prioritized genes are always  
76 within the CeD-associated regions.

77 **Mediating cis gene** – a prioritized gene that is statistically responsible for the change in  
78 expression of a trans-eQTL gene. Of note, while the trans-eQTL is located in the same CeD-  
79 associated region of the mediating cis-gene, the mediated trans-gene is not.

80 **Mediated trans gene** – a gene located outside CeD-associated regions that is statistically  
81 mediated by a mediating cis gene located in the same region of the corresponding trans-  
82 eQTL.

83

## 84 Introduction

85

86 Celiac disease (CeD) is an auto-immune disease in which patients experience severe  
87 intestinal inflammation upon ingestion of gluten peptides. CeD has a large genetic  
88 component, with heritability estimated to be approximately 75%<sup>1</sup>. The largest CeD-impacting  
89 locus is the HLA region, which contributes approximately 40% of CeD heritability<sup>2</sup>. While the  
90 individual impacts of CeD-associated genes outside the HLA region are smaller, they jointly  
91 account for an additional 20% of heritability. Previous genome-wide association studies  
92 (GWAS) have identified 42 non-HLA genomic loci associated with CeD<sup>3–6</sup>, but the biological  
93 mechanisms underlying the association at each locus and the genes involved in disease  
94 susceptibility are largely unknown. Yet, identification of these non-HLA genetic components  
95 and an understanding of the molecular perturbations associated with them are necessary to  
96 understand CeD pathophysiology.

97 Understanding the biological mechanisms of non-HLA CeD loci is difficult: only three  
98 of these loci point to single nucleotide polymorphisms (SNPs) located in protein-coding  
99 regions<sup>3</sup>. The other CeD-risk loci cannot be explained by missense mutations, making it  
100 necessary to look at other biological mechanisms such as gene expression to explain their  
101 role in CeD pathogenicity. Several studies have been performed to integrate expression  
102 quantitative trait loci (eQTLs) with CeD GWAS associations<sup>4,7,8</sup>, and several candidate  
103 genes, including *UBASH3A*, *CD274*, *SH2B3* and *STAT4*<sup>9</sup>, have been pinpointed, implicating  
104 T cell receptor, NFκB and interferon signalling pathways as biological pathways associated  
105 with CeD pathology. Unfortunately, these eQTL studies had limited sample sizes, which  
106 reduced their power to identify *cis*- and (especially) *trans*-eQTLs. Furthermore, previous  
107 attempts to integrate eQTLs have mostly annotated genomic loci based on catalogued  
108 eQTLs without formally testing the causality of the genes in the onset or exacerbation of  
109 CeD<sup>8,10,11</sup>.

110 Gene expression and GWAS data can also be integrated using methodologies that  
111 identify shared mechanisms between diseases. These methods can be roughly divided into  
112 three classes: variant colocalization methods, causal inference methods and co-expression  
113 methods. Colocalization methods consider the GWAS and eQTL summary statistics at a  
114 locus jointly and probabilistically test if the two signals are likely to be generated by the same  
115 causal variant<sup>12</sup>. Causal inference methods test if there is a causal relationship between  
116 expression changes and the disease, using genetic associations to remove any  
117 confounders<sup>13,14</sup>. Finally, co-expression methods do not use eQTL information, but rather  
118 test if there is significant co-expression between the genes that surround the GWAS locus<sup>15</sup>.

119 Unfortunately, there is no current “gold standard” method for finding the causal gene behind  
120 a GWAS hit, as all the methods discussed here are subject to their respective assumptions,  
121 drawbacks and caveats. However, it is worthwhile to use all these methods in parallel to find  
122 the most relevant causal genes for CeD.

123 Here, we systematically applied all four methods to the latest meta-analysis results  
124 for CeD<sub>5</sub> and coupled them with eQTL results from the Biobank Integrative Omics Study  
125 (BIOS) cohort<sup>16</sup>, one of the largest cohorts for which there is genotype and RNA-seq  
126 expression data of peripheral blood mononuclear cells (schematic overview **Fig. 1A-B**). We  
127 focused on 58 GWAS loci that showed significant association with CeD at  $p < 5 \times 10^{-6}$ . Our  
128 approach prioritized 118 genes in 50 loci and identified one gene, *TRAFD1*, as a master  
129 regulator of *trans*-effects. We then experimentally validated the role of *TRAFD1*-mediated  
130 genes using RNA-seq in a disease-relevant cell type. Our study yields novel insights into the  
131 genetics of CeD and is proof-of-concept for a systematic approach that can be applied to  
132 other complex diseases.

133

## 134 **Methods**

135

### 136 **Genotypes for eQTL analysis**

137 We used the BIOS cohort<sup>16</sup> to map eQTLs in 3,746 individuals of European ancestry. The  
138 BIOS cohort is a collection of six cohorts: the Cohort on Diabetes and Atherosclerosis  
139 Maastricht<sup>17</sup>, the Leiden Longevity Study<sup>18</sup>, Lifelines DEEP<sup>19</sup>, the Netherlands Twin  
140 Registry<sup>20</sup>, the Prospective ALS Study Netherlands<sup>21</sup> and the Rotterdam Study<sup>22</sup>. As  
141 described in Vosa et al.<sup>23</sup>, each cohort was genotyped separately using different arrays.  
142 Genotypes were subsequently imputed to the Haplotype Reference Consortium panel (HRC  
143 v1.0) on the Michigan imputation server<sup>24</sup>.

144 We considered only biallelic SNPs with a minor allele frequency (MAF)  $> 0.01$ , a  
145 Hardy-Weinberg test  $p$  value  $> 10^{-6}$  and an imputation quality RSQR  $> 0.8$ . To remove  
146 related individuals, a genetic relationship matrix (GRM) was created using plink 1.9<sup>25</sup>  
147 (command `--make-grm-bin`) on linkage disequilibrium (LD)-pruned genotypes (option: “`--`  
148 `indep 50 5 2`”). Pairs of individuals with a GRM value  $> 0.1$  were considered related, and one  
149 individual was removed from each of these pairs. Population outliers were identified using a  
150 principal component analysis on the GRM, and we removed individuals who were more than  
151 3 standard deviations from the means of principal component 1 or 2.

152

## 153 **Expression quantification**

154 We used the same procedure for RNA gene expression control and processing as described  
155 in Zhernakova et al.<sup>16</sup> In brief, RNA was extracted from whole blood and paired-end  
156 sequenced using the Illumina HiSeq 2000 machine. Read alignment of RNA-seq reads was  
157 done using STAR (v2.3.0)<sup>26</sup> using a reference genome with masked variants with MAF <  
158 0.01 in the Genome of the Netherlands<sup>27</sup>. Aligned reads were quantified using HTSeq<sup>28</sup>.  
159 Samples were removed if they had fewer than 80% aligned reads, fewer than 85% exon-  
160 mapping reads, or if they had a median 3' bias larger than 70% or smaller than 45%.  
161 Unobserved expression confounders were removed following the procedure of Zhernakova  
162 et al.<sup>16</sup>, correcting the expression matrix for the first 25 principal components as well as 3'  
163 bias, 5'bias, GC content, intron base pair percentage and sex.

164

## 165 **eQTL analysis**

166 After genotype and RNA-seq quality controls (QCs), 3,503 individuals, 19,960 transcripts  
167 and 7,838,327 autosomal SNPs remained for analyses. We performed genome-wide eQTL  
168 mapping for the transcripts using plink 1.9<sup>25</sup> with the --assoc command. We defined *cis*-  
169 eQTL variants as those located within  $\pm 1.5$ Mb of the transcript and *trans*-eQTLs as variants  
170 located outside these boundaries. To select variants that could explain the *cis*-eQTL signal  
171 of a gene, we used GCTA-COJO software<sup>29</sup> v1.26. For this analysis, we required selected  
172 variants to reach a *p*-value threshold of  $5 \times 10^{-6}$  and included the BIOS cohort genotypes as  
173 LD reference. This identified 707 genes with at least one eQTL reaching this threshold, 357  
174 of which had more than one conditionally independent eQTL variant.

175

## 176 **CeD summary statistics associated regions and candidate genes**

177 We used summary statistics from a CeD GWAS meta-analysis of 12,948 cases and 14,826  
178 controls that analysed 127,855 variants identified using the Immuchip arrays<sup>5</sup>. SNP  
179 positions were lifted over to human genome build 37 using the UCSC liftover tool. We first  
180 identified lead associated variants in the CeD meta-analysis by performing *p*-value clumping:  
181 we used plink 1.9<sup>25</sup> to select variants at a *p*-value threshold of  $5 \times 10^{-6}$  and pruned variants in  
182 LD with these selected variants using standard plink settings ( $R_2 > 0.5$ , utilizing 1000  
183 Genomes European sample LD patterns)<sup>25,30</sup>. We removed variants in an extended HLA  
184 region (chromosome 6, 25Mb to 37Mb) due to the complex long range LD structure in this  
185 region and because we aim to understand the function of the non-HLA genetic component of  
186 CeD. We looked for candidate genes around the clumped variants as follows. First, we

187 defined regions around every clumped variant by padding the clumped SNP position by 1Mb  
188 on both sides. We then joined all overlapping CeD-associated regions together and looked  
189 for gene transcripts that partly or fully overlapped with the associated regions. This approach  
190 identified 58 CeD-associated regions and 1,235 candidate genes that are potentially causal  
191 for CeD. Of note, the CeD-association windows were set to be smaller than the eQTL  
192 window so that eQTL associations would fully overlap the associated CeD GWAS peak even  
193 when a gene is on the edge of the CeD-associated region.

194

### 195 **Gene prioritization using Mendelian Randomization–Inverse Variance Weighting (MR- 196 IVW), COLOC, LD overlap and DEPICT**

197 We prioritized CeD-associated genes using three eQTL-based methods – MR-IVW<sup>31</sup>,  
198 COLOC<sup>12</sup> and LD overlap – and one co-regulation-based method, DEPICT<sup>15</sup>. For the MR-  
199 IVW method, we used the independent variants identified by GCTA-COJO as instrumental  
200 variables<sup>13,32</sup> to test causal relationships between changes in gene expression and CeD.  
201 MR-IVW was only performed when there were three or more independent eQTLs available  
202 (164 genes). A gene was significant for the MR-IVW test if the causal estimates passed a  
203 Bonferroni threshold  $p$ -value of  $3.1 \times 10^{-4}$ . Heterogeneity of causal estimates was accounted  
204 for and corrected for using Weighted Median MR analysis and Cochran's Q test<sup>33</sup>. For the  
205 COLOC method, we used the 'coloc' R package and considered a gene significant for the  
206 COLOC analysis if the posterior probability of shared variants (H4) was larger than 0.9. For  
207 the LD overlap method, a gene was considered significant if there was high LD ( $r_2 > 0.8$ )  
208 between the top independent eQTL and the top CeD variant in the region. Finally, we  
209 applied DEPICT<sup>15</sup> to the clumped CeD GWAS variants described in 'CeD summary statistics  
210 associated regions and candidate genes'. Genes identified by the DEPICT analysis were  
211 considered significant if a False Discovery Rate (FDR)  $< 0.05$  was found with DEPICT's own  
212 permutation measure.

213 We scored each gene in the CeD-associated loci by considering each of the four  
214 prioritization methods. A gene was prioritized as 'potentially causal' in CeD pathology when  
215 one of the four methods was significant (one line of evidence). If multiple lines of evidence  
216 were significant, the gene was prioritized more highly than when only a single line of  
217 evidence was available.

218 To explore how the prioritized genes affect CeD risk, we gave each gene an effect  
219 direction based on the effect direction of the top variants in the eQTL and the CeD GWAS  
220 using the following algorithm:



- 221 1. If there was a concordant effect that was significant in the top variants of both the  
222 eQTLs and the GWAS, the direction of the concordant effect was chosen.
- 223 2. If there was a concordant effect, but no significance of the SNP in one of the  
224 datasets, we could not be sure of an effect direction, and a question mark was  
225 chosen. The only exception to this was if the MR-IVW was significant, when we  
226 chose the direction of the MR-IVW effect.
- 227 3. If there was a discordant effect between the top SNPs, and both were significant in  
228 both datasets, a question mark was chosen. The only exception to this was when the  
229 IVW was significant, when the IVW effect was chosen.
- 230 4. If there was a discordant effect and there was significance in only one of the GWAS  
231 from the eQTL top SNP, the eQTL direction was chosen.
- 232 5. If there was a discordant effect and there was significance in only one of the eQTL  
233 from the GWAS top SNP, the GWAS direction was chosen.
- 234 6. If there was otherwise a discordant effect, a question mark was chosen.

235 Each gene is given a mark: positive ('+'), negative ('-') or unknown ('?'). '+' indicates that  
236 increased expression increases CeD risk. '-' indicates that increased expression decreases  
237 CeD risk. '?' indicates that it is unknown how the expression affects CeD risk.

### 238 **Co-regulation clustering**

239 The genes that have been prioritized may have some shared function in CeD pathology. To  
240 identify possible shared pathways, we performed co-regulation clustering analysis based on  
241 1,588 normalized expression co-regulation principal components identified from RNA-seq  
242 information across multiple human tissues by Deelen et al<sup>34</sup>. We performed pairwise  
243 Pearson correlation of our prioritized genes with these 1,588 principal components and  
244 derived a correlation Z score for each prioritized gene pair. We then performed hierarchical  
245 clustering of this Z score matrix using Ward distances and identified 4 clusters from the  
246 resulting dendrogram.

### 247 **Trans eQTL and mediation analysis**

248 238 autosomal genes that were not located in, but were associated with, a significant *trans*-  
249 eQTL variant ( $p < 5 \times 10^{-8}$ ) in the CeD-associated regions were identified and used as  
250 potential targets for mediation by our associated genes in the CeD-associated loci (86  
251 potential *cis* mediating genes). We first selected *trans*-eQTL genes that were co-expressed  
252 (Pearson  $r > 0.1$ , 197 gene combinations) with prioritized genes, then performed mediation  
253 analysis by running the *trans*-eQTL association again using the expression of the *cis*-eQTL  
254 gene as a covariate. We defined a *trans*-mediated gene if, after mediation analysis, the  
255 change (increase or decrease) in the effect size of the top *trans*-eQTL variant was significant



256 according to the statistical test described in Freedman and Schatzkin<sup>35</sup>. For this analysis, we  
257 used a Bonferroni-adjusted  $p$ -value of  $3.0 \times 10^{-4}$ .

### 258 **Cell type proportion and *SH2B3* expression mediation analysis**

259 To assess if the *cis*-eQTL effect of *TRAFD1* was not a proxy for cell-type composition, we  
260 performed mediation analyses in a fashion similar to the *trans* mediation analysis above  
261 using cell proportions measured in a subset of individuals in the BIOS cohort. To ensure that  
262 there was no residual effect of *SH2B3*-expression on the mediating effect of *TRAFD1*, we  
263 corrected the original *TRAFD1* expression levels for the expression levels of *SH2B3*, leaving  
264 *TRAFD1* expression independent of *SH2B3*, and reran the mediation analysis.

265 **Literature review.** We performed a REACTOME pathway<sup>36</sup> analysis to determine the  
266 potential function of the prioritized genes. This was complemented with a literature search  
267 (research and review papers) in Pubmed. For the coding and non-coding genes for which no  
268 studies were found, Genecards ([www.genecards.org](http://www.genecards.org)) and Gene Network v2.0 datasets  
269 ([www.genenetwork.nl](http://www.genenetwork.nl))<sup>34</sup> were used, respectively. Information regarding the potential  
270 druggability of the prioritized genes was obtained from DrugBank<sup>37</sup>, the pharmacogenetics  
271 database<sup>38</sup> and a previous study that catalogued druggable genes<sup>39</sup>.

272 **THP-1 culture.** The cell line THP-1 (Sigma Aldrich, ECACC 88081201) was cultured in  
273 RPMI 1640 with L-glutamine and 25mM HEPES (Gibco, catalogue 52400-025), and  
274 supplemented with 10% fetal bovine serum (Gibco, catalogue 10270) and 1% penicillin/  
275 streptomycin (Lonza, catalog DE17602E). The cells were passed twice per week at a  
276 density lower than  $0.5 \times 10^6$  cells/ml in a humidified incubator at 5% CO<sub>2</sub>, 37°C.

277 **siRNA treatment.** THP-1 cells were plated at  $0.6 \times 10^6$  cells/ml and transfected with 25 nM  
278 siRNA using Lipofectamine RNAiMax transfection reagent (Invitrogen, catalogue 13788),  
279 according to the manufacturer's protocol. Cells were treated with an siRNA to target  
280 *TRAFD1* (Qiagen catalogue 1027416, sequence CCCAGCCGACCCATTAACAAT)  
281 (Knockdown (KD)), and cells treated with transfection mix without siRNA (Wild type (WT)) or  
282 non-targeting control siRNA (scrambled (SCR)) (Qiagen catalog SI03650318, sequence  
283 undisclosed by company) were included as controls. All the treatments were performed in  
284 triplicate. 72 hours after transfection, a small aliquot of cells was stained for Trypan Blue  
285 exclusion to determine cell viability and proliferation. The cells were stimulated with either  
286 LPS (10 ng/ml) from *E. coli* (Sigma catalogue 026:B6) or media alone (unstimulated) for 4h.  
287 Subsequently, the cells were centrifuged, and the cell pellets suspended in lysis buffer and  
288 stored at -80°C until used for RNA and protein isolation.

289 **qPCR.** The total RNA from THP-1 cells was extracted with the mirVana™ miRNA isolation  
290 kit (AMBION, catalogue AM1561) and subsequently converted to cDNA using the RevertAid  
291 H Minus First Strand cDNA Synthesis Kit (Thermo scientific, catalogue K1631). qPCR was  
292 done using the Syber green mix (Bio-Rad, catalogue 172-5124) and run in a QuantStudio 7  
293 Flex Real-Time system (Applied Biosystems, catalogue 448598). Primer sequences to  
294 determine KD levels of *TRAFD1* were 5' GCTGTAAAGAAGCATGAGGAGAC and 3'  
295 TTGCCACATAGTTCCGTCCG. *GAPDH* was used as endogenous qPCR control with  
296 primers 5' ATGGGGAAGGTGAAGGTCG and 3' GGGGTCATTGATGGCAACAATA.  
297 Relative expression values of *TRAFD1* were normalized to the endogenous control *GAPDH*  
298 and calculated using the  $\Delta\Delta CT$  method, then given as a percentage relative to SCR  
299 expression levels.

300 **Western blot (WB).** Cell pellets from THP-1 cells were suspended on ice-cold lysis buffer  
301 (PBS containing 2% SDS and complete protease inhibitor cocktail (Roche, catalog  
302 11697498001)). Protein concentration of cell extracts was determined using the BCA protein  
303 kit (Pierce, catalog 23225). Proteins were separated on 10% SDS-polyacrylamide  
304 electrophoresis gel and transferred to a nitrocellulose membrane. After 1 hour of blocking  
305 with 5% fat-free milk in Tris-Tween-Buffer-Saline, the membranes were probed for 1 hour at  
306 room temperature with mouse mono-clonal TRAFD1 antibody 1:1000 (Invitrogen, catalog  
307 8E6E7) or mouse monoclonal anti-actin antibody 1:5000 (MP Biomedicals, catalog  
308 08691001), followed by incubation with goat anti-mouse horseradish peroxidase–conjugated  
309 secondary antibodies 1:10000 (Jackson Immuno Research, catalog 115-035-003). After  
310 three 10-minute washes, the bands were detected by Lumi light WB substrate (Roche,  
311 catalogue 12015200001) in a Chemidoc MP imaging system (Bio-Rad) and quantified using  
312 Image Lab™ software (Bio-Rad). The band intensity of TRAFD1 was normalized to actin,  
313 and the TRAFD1 SCR control level was set as 100%.

314 **Statistical analysis for *in vitro* experiments in THP-1 cells.** The statistical analyses of  
315 proliferation, qPCR and WB were performed using Prism 5 software (GraphPad Software,  
316 Inc.). Results are presented as mean  $\pm$  SEM from a representative experiment. Statistical  
317 differences were evaluated using a one-tailed *t*-test.

318 **RNA sequencing (RNA-seq) in THP-1 cells.** RNA from THP-1 cells was extracted with the  
319 mirVana™ miRNA isolation kit (AMBION, catalog AM1561). Prior to library preparation,  
320 extracted RNA was analysed on the Experion Stdsend RNA analysis kit (Bio-Rad, catalog  
321 7007105). 1  $\mu$ g of total RNA was used as input for library preparation using the quant seq 3'  
322 kit (Lexogen, catalog 015.96), according to the manufacturer's protocol. Each RNA library  
323 was sequenced on the Nextseq500 (Illumina). Low quality reads, adaptors and poly-A tail

324 reads were removed from FASTQ files. The QC-ed FASTQ files were then aligned to the  
325 human\_g1k\_v37 Ensembl Release 75 reference genome using HISAT default settings<sup>40</sup>,  
326 and sorted using SAMtools<sup>41</sup>. Gene-level quantification was performed by the featurecounts  
327 function of the RSubread R package v1.6.2<sup>42</sup>. A modified Ensembl version 75 gtf file mapping  
328 only to the last 5' 500 bps per gene was used as gene-annotation database to prevent  
329 counting of reads mapping to intra-genic A-repeats. Gene-level differential expression  
330 analysis between conditions was performed using the DESeq2 R package<sup>43</sup> after removing  
331 genes with zero counts. Differentially expressed genes (DEGs) were defined as genes  
332 presenting an absolute log<sub>2</sub> fold change ( $|\log_2 \text{FC}| > 1$ ) and an FDR  $\leq 0.01$  across treatment  
333 (WT vs. SCR or KD unstimulated cells). To identify the genes responding to LPS stimulation,  
334 the DEGs between unstimulated samples and their respective stimulated sample were  
335 determined. Venn diagrams were used to depict the relationship between these genes.  
336 REACTOME pathway analyses were performed to identify biological processes and  
337 pathways enriched in different sets of DEGs using the enrichr API. Enrichments were  
338 considered significant if they were below a 0.05 FDR-threshold defined by the enrichr API<sup>36</sup>.

339 **Gene set permutation analysis.** It can be difficult to determine if a set of genes is 'on  
340 average' more or less differentially expressed due to co-expression between the genes  
341 within the set. To mitigate this, we performed a permutation test that considers the median  
342 absolute T statistic calculated by DESeq2<sup>43</sup> in the WT-SCR experiment as a null observation  
343 and compared this null observation with the SCR-KD experimental comparison. This allowed  
344 us to compare the expected differential expression of a set of genes, based on the WT-SCR  
345 comparison, with the observed differential expression of the same set of genes in the SCR-  
346 KD comparison, while still incorporating the co-expression structure of the data. To do this,  
347 we randomly selected a same-sized set of genes 1,000,000 times in each relevant  
348 experiment (WT-SCR or SCR-KD), and determined the observed median absolute T  
349 statistic. We calculated a ratio of how often the permuted value is higher than the observed  
350 value. For example, the observations can be that 1% of permuted gene sets are more  
351 differentially expressed in the WT-SCR experiment, while only 0.01% of permuted genes  
352 sets are more differentially expressed in the SCR-KD experiment. Finally, we divide these  
353 values by one another, (percentage SCR-KD)/(percentage WT-SCR), to calculate a fold  
354 increase in differential expression. In the example given above, this indicates that the KD is  
355 100 times ( $0.01/1 = 100$ ) more differentially expressed than expected.

356 **Available RNA-seq datasets.** Four available RNA-seq datasets were included to study the  
357 pattern of expression of prioritized genes. A brief description of each dataset is provided  
358 below. (GEO submission in process).

359 **Whole biopsy samples.** Duodenal biopsies were obtained from 11 individuals (n=6 CeD  
360 patients and n=5 controls) who underwent upper gastrointestinal endoscopy (previously  
361 described)<sup>44</sup>. All individuals gave informed consent. To identify DEGs between patients and  
362 controls, a filter of  $|\log_2 FC| > 1$  and  $FDR \leq 0.05$  was applied using the DESeq2 R package.

363 **Intra epithelial cytotoxic lymphocytes (IE-CTLs).** CD8<sup>+</sup> TCR $\alpha\beta$  IE-CTLs cell lines were  
364 isolated from intestinal biopsies and expanded for 12 days, as described previously<sup>45</sup>. Cells  
365 were left unstimulated (controls) or treated for 3 hours with IFN $\beta$  (300 ng/ml, Pbl Assay  
366 science, cat 11410-2), IL-15 (20 ng/ml, Biolegend, cat 570304) or IL-21 (3 ng/ml, Biolegend,  
367 cat 571204) (n=8 samples per condition, as previously reported)<sup>44</sup>. Differential expression  
368 analysis between unstimulated cells and cytokine-treated IE-CTLs was performed using the  
369 R package DESeq2. DEGs were defined as genes presenting a  $|\log_2 FC| > 1$  and an  $FDR \leq$   
370 0.05 between untreated controls and cytokine-treated samples.

371 **Gluten specific (gs) CD4<sup>+</sup> T cells.** gsCD4<sup>+</sup> T cell lines were generated from intestinal  
372 biopsies and expanded for 2 weeks, as reported previously<sup>46</sup>. Cells were stimulated for 3  
373 hours with 2.5  $\mu\text{g/ml}$  of anti-CD3 (Biolegend, catalog 317315) and anti-CD28 (Biolegend,  
374 catalog 302923) antibodies. Untreated cells were included as control. N=22 samples per  
375 condition. DEGs were extracted with the DESeq2 package using the cut-off of  $|\log_2 fc| > 1$  and  
376  $FDR \leq 0.05$  between unstimulated samples and controls.

377 **Caco-2 cells.** After 2 weeks of expansion in Transwells, the cells were treated with 60 ng/ml  
378 of IFN $\gamma$  (PeproTech) for 3 hours. Untreated cells were included as controls. RNA samples  
379 were extracted and further processed for RNA-seq (as described previously<sup>44</sup>). DEGs  
380 between control and stimulated cells were extracted with the DESeq2 R package using a  
381 cut-off of  $|\log_2 FC| > 1$  and  $FDR \leq 0.05$ .

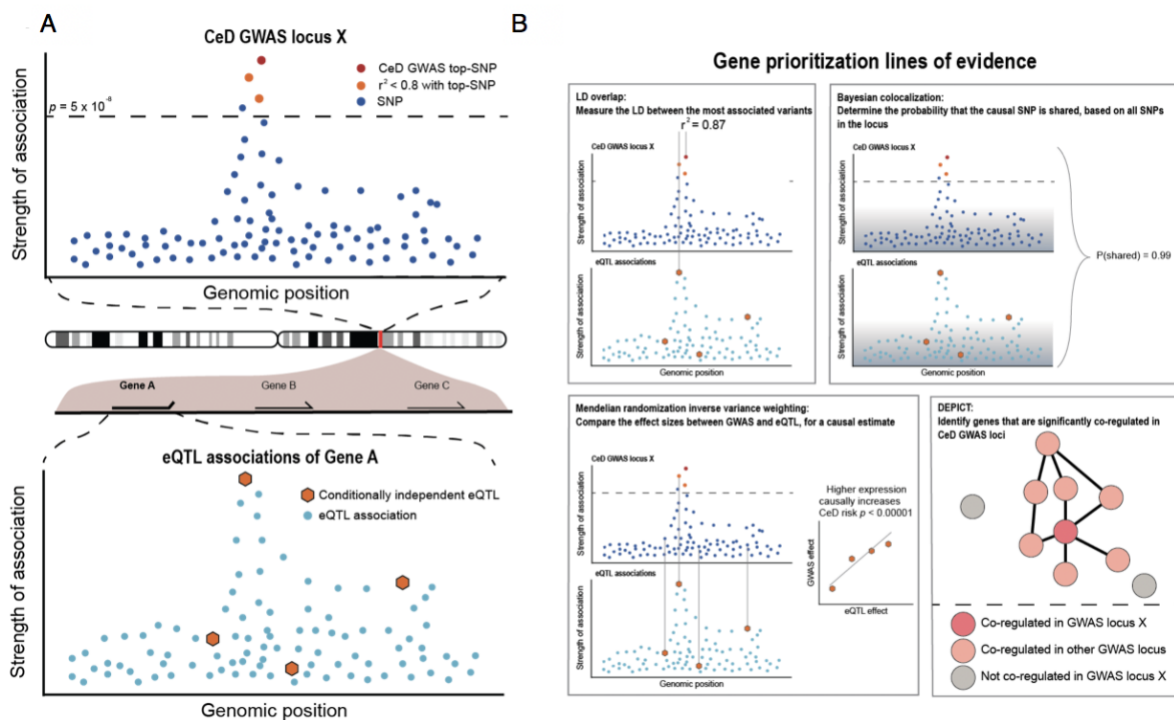
382

## 383 **Results**

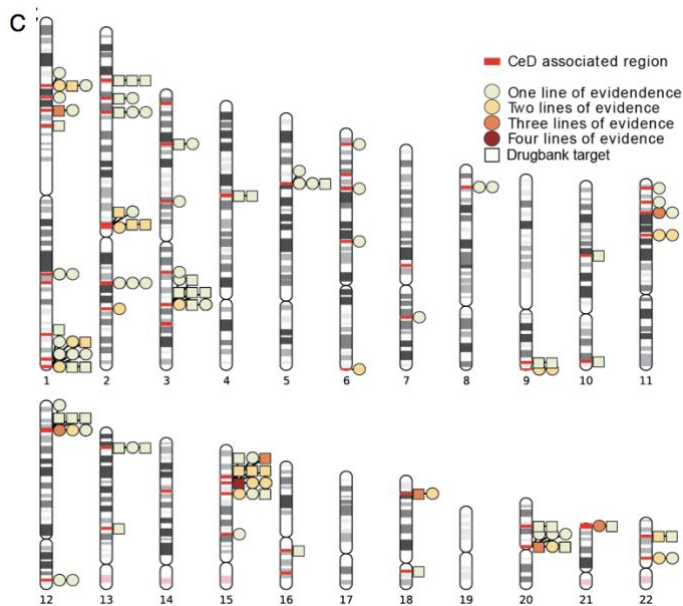
### 384 **Gene prioritization identifies 118 likely causal CeD genes.**

385 To identify genes that most likely play a role in CeD (prioritized genes), we combined a  
386 recent genome-wide association meta analysis<sup>5</sup> with (1) eQTLs derived from whole-blood  
387 transcriptomes of 3,503 Dutch individuals<sup>16</sup> and (2) a co-regulation matrix derived from  
388 expression data in multiple different tissues and 77,000 gene expression samples<sup>15</sup>. We  
389 selected 1,258 genes that were within 1Mb of the 58 CeD-associated non-HLA variant  
390 regions ( $p < 5 \times 10^{-6}$ ) (see Methods), and prioritized the genes that are the most likely  
391 causally related to CeD using four different gene prioritization methods: MR-IVW<sup>13</sup>,  
392 COLOC<sup>12</sup>, LD overlap and DEPICT<sup>15</sup> (**Fig. 1A-B**) (**Supplementary Table 1**).

393



394



395

396 **Fig. 1 Cis-eQTL prioritized candidate genes in CeD loci.** (A) A CeD GWAS association curve at a  
 397 hypothetical GWAS locus X and the eQTL association at a potential candidate gene A. In both  
 398 association plots, each dot represents a SNP plotted against the genomic position (X axis) and the  
 399 strength of association (Y axis). In the GWAS association curve, the top SNP is marked in red, while  
 400 other SNPs above the significance threshold (dashed line) are coloured according to their LD with the  
 401 top SNP. In the eQTL association curve, independent eQTLs are marked in red. (B) A conceptual  
 402 depiction of the four statistical methods applied to link a disease locus to an eQTL locus. (C) A  
 403 chromosome ideogram depicting the location of each prioritized gene identified in a CeD-associated  
 404 GWAS locus. Loci are marked with red bars. Genes depicted by a square are the target of an  
 405 approved drug or a drug in development. All other genes are depicted by a circle. Each circle or  
 406 square is coloured according to the lines of evidences supporting its causal role.

407



408 The first method we applied, MR-IVW, is a two-sample Mendelian Randomization  
409 approach called inverse variance weighting (see **Methods**). Our MR-IVW used summary  
410 statistics from two datasets: the eQTL and CeD GWAS. First, independent eQTLs at a locus  
411 were identified (see **Methods**), then the effect sizes of the eQTL and the GWAS were  
412 combined to identify gene expression changes that are causal (or protective) for CeD<sub>13,14</sub>  
413 (see **Methods**). We only applied this method to a subset of 162 genes for which at least  
414 three independent *cis*-eQTL variants (at  $p < 5 \times 10^{-6}$ ) were identified (see **Methods**)<sup>32</sup>. We  
415 accounted for heterogeneity using the Q test and weighted median method and found that  
416 the effect sizes were very similar before and after correction (**Supplementary Table 2**).

417 The second method, COLOC, is a variant colocalization test in which we used eQTL  
418 and CeD summary statistics for all the SNPs in a locus and Bayesian probability to infer  
419 whether the eQTL and the CeD-association signals are likely to originate from the same  
420 causal variant<sup>12</sup>.

421 The third method, LD overlap, is a more classical annotation-type approach that  
422 prioritizes a gene if the top eQTL is in strong LD ( $r_2 > 0.8$ ) with the variant most significantly  
423 associated with CeD in a locus. This and the COLOC method were applied to 707 genes for  
424 which at least one significant eQTL variant was found.

425 Finally, we used DEPICT<sup>15</sup>, a gene-prioritization method based on co-regulation in  
426 expression datasets across multiple different tissues. DEPICT identifies enrichment for co-  
427 regulated genes from genes in a GWAS locus. In contrast to the other methods, DEPICT  
428 assessed the potential role of all 1,258 genes independently of the presence of an eQTL.

429 In total, 118 out of the 1,258 assessed genes were prioritized by at least one of the  
430 four methods. Of these 118 genes, 28 had two lines of evidence, 7 genes (*CD226*, *NCF2*,  
431 *TRAFD1*, *HM13*, *COLCA1*, *CTSH*, *UBASH3A*) had three lines of evidence, and one gene  
432 (*CSK*) was supported by all four methods (**Supplementary Table 1**) (**Fig. 1C**). Overall, we  
433 identified potentially causal genes in 50 out of 58 CeD-associated regions.

434 The four different gene prioritization methods complement each other in different  
435 ways. DEPICT prioritized the most genes: 66 in total, 38 of them uniquely prioritized (38/66,  
436 58% unique). One reason for this is that DEPICT is based on co-expression, not genetic  
437 background. Indeed, 16 genes prioritized by DEPICT do not have a significant eQTL  
438 associated with them. Overall, the most concordance was found between COLOC and LD  
439 overlap (30% and 26% unique genes, respectively) as these methods are the most similar,  
440 while MR-IVW uniquely prioritized a relatively large proportion of genes (9/20, 45% unique).  
441 Thus, each method helps prioritize genes with multiple lines of evidence, but also adds a  
442 unique set of genes based on the assumptions of the method.

443 To see if any of these genes could lead to therapeutic intervention in CeD, we  
444 searched for the CeD-associated genes in DrugBank and assessed their druggability

445 potential following Finan et al.<sup>39</sup> (**Supplementary Table 3**). 26 of the 118 prioritized genes  
446 encode proteins that are targeted by an approved drug or a drug in development according  
447 to drugbank (**Fig. 1C**) (**Supplementary Table 3**). For example, drugs such as Natalizumab  
448 and Basiliximab that target the proteins encoded by *ITGA4* and *IL21R*, respectively, are  
449 currently approved or under study for the treatment of immune-mediated diseases including  
450 rheumatoid arthritis<sup>47</sup>, Crohn's disease<sup>48</sup> and multiple sclerosis<sup>49</sup> or as an immune-  
451 suppressor to avoid kidney transplant rejection. An additional 25 genes encode proteins that  
452 are similar to proteins targeted by already approved drugs following Finan et al.<sup>39</sup>  
453 (**Supplementary Table 3**).

454

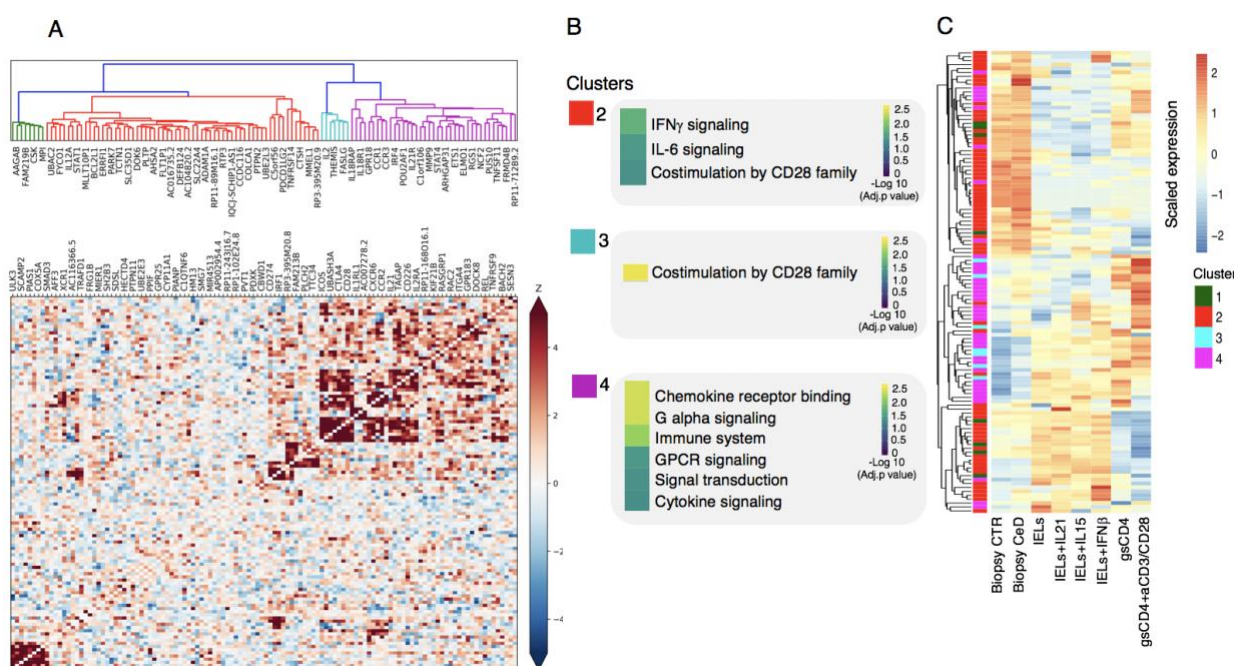
### 455 **Co-expression patterns of *cis*-eQTL-prioritized loci reveal four functional clusters**

456 The biological function for the 118 prioritized genes and their role in CeD pathology is not  
457 fully understood. We sought to infer biological function using a guilt-by-association co-  
458 regulation approach to identify clusters of shared molecular function (see **Methods**). We  
459 identified co-regulated genes by correlating our prioritized gene list in 1,588 principal  
460 components that were identified from the co-expression of 31,499 RNA-seq samples across  
461 multiple tissues<sup>34</sup> (**Fig. 2A**). We then performed REACTOME 2016 gene set enrichment<sup>36</sup>  
462 analysis to investigate the biological processes enriched in each cluster (**Supplementary**  
463 **Table 4**) (**Supplementary Table 5**).

464 We could not identify a specific biological process linked to our first co-regulation  
465 cluster. However, genes such as *ULK3* (relevant for autophagy<sup>50</sup>) and *CSK* (relevant to T  
466 cell receptor (TCR) signaling<sup>51</sup>) are included in this co-regulation cluster. Our second cluster  
467 encompasses genes (e.g. *STAT1*, *CD274* and *IL12A*) implicated in interferon gamma (IFN $\gamma$ )  
468 signalling and interleukin (IL)-6 signalling. Co-regulation cluster 3 contains genes (e.g.  
469 *CD28*, *CTLA4* and *ICOS*) associated with co-stimulation by CD28, a process that is  
470 essential for modulating T cell-activation. Finally, co-regulation cluster 4 contains chemokine  
471 (e.g. *CCR1*, *CCR2* and *CCR3*) and cytokine signalling genes (e.g. *IL2RA*, *IL21* and *IL18R1*)  
472 (**Fig. 2B**). The biological processes overrepresented in these co-regulation clusters are  
473 essential for the activation and function of the adaptive and innate immune system, which  
474 confirms and extends previous findings that implicate both arms of the immune system in  
475 CeD disease pathogenesis. Approximately 10% of the prioritized genes are long non-coding  
476 RNAs (lncRNAs) rather than protein-coding genes (**Supplementary Table 1**). Although little  
477 is known about the function of lncRNAs, their co-regulation pattern with the genes in clusters  
478 2 and 4 suggests that they may be associated with cytokine/chemokine signalling (**Fig. 2A,**  
479 **B**). Moreover, by using Genenetwork<sup>34</sup>, we found that the lncRNAs *RP3-395M20.9*,  
480 *AC007278.2* and *AC104820.2* may be involved in tumour necrosis factor (TNF) signalling,  
481 neutrophil degranulation and chemokine receptor signalling, respectively, implying a role for  
482 these uncharacterized lncRNAs in immune regulation in CeD.

483





484  
 485 **Fig. 2 Co-expression pattern of *cis*-eQTL prioritized genes reveals four functional**  
 486 **clusters.** (A) Heatmap showing the Spearman correlations between gene expression patterns of  
 487 each prioritized gene. Blue squares indicate negative correlation. Red squares indicate positive  
 488 correlation. Both are shaded on a gradient scale according to the Z score of the correlation. A  
 489 dendrogram computed with Ward distances between the correlations is shown on top of the  
 490 heatmap. Branches of the dendrogram are coloured differently to mark separate clusters. (B)  
 491 Results of the REACTOME gene set enrichment analysis of the genes belonging to each of the  
 492 clusters identified in (A). Colour key denotes the significance ( $-\log_{10}$  multiple testing adjusted  $p$   
 493 value) of each biological pathway. (C) Heatmaps depicting the scaled expression of prioritized  
 494 genes belonging to the four clusters identified in (A) in three available RNA-seq datasets:  
 495 intestinal biopsies from controls (CTR,  $n=5$  samples) or CeD patients (CeD,  $n=6$  samples); CD8+  
 496 TCR $\alpha\beta$  intraepithelial cytotoxic lymphocytes (IE-CTLs) unstimulated or treated with IL-21, IL-15  
 497 or IFN $\beta$  for 3 hours ( $n=8$  samples per condition) and gsCD4+ T cells unstimulated or treated  
 498 with anti-CD3 and anti-CD28 (aCD3) for 3 hours ( $n=22$  samples per condition). Clustering was  
 499 performed using the “average” method in hclust().

500

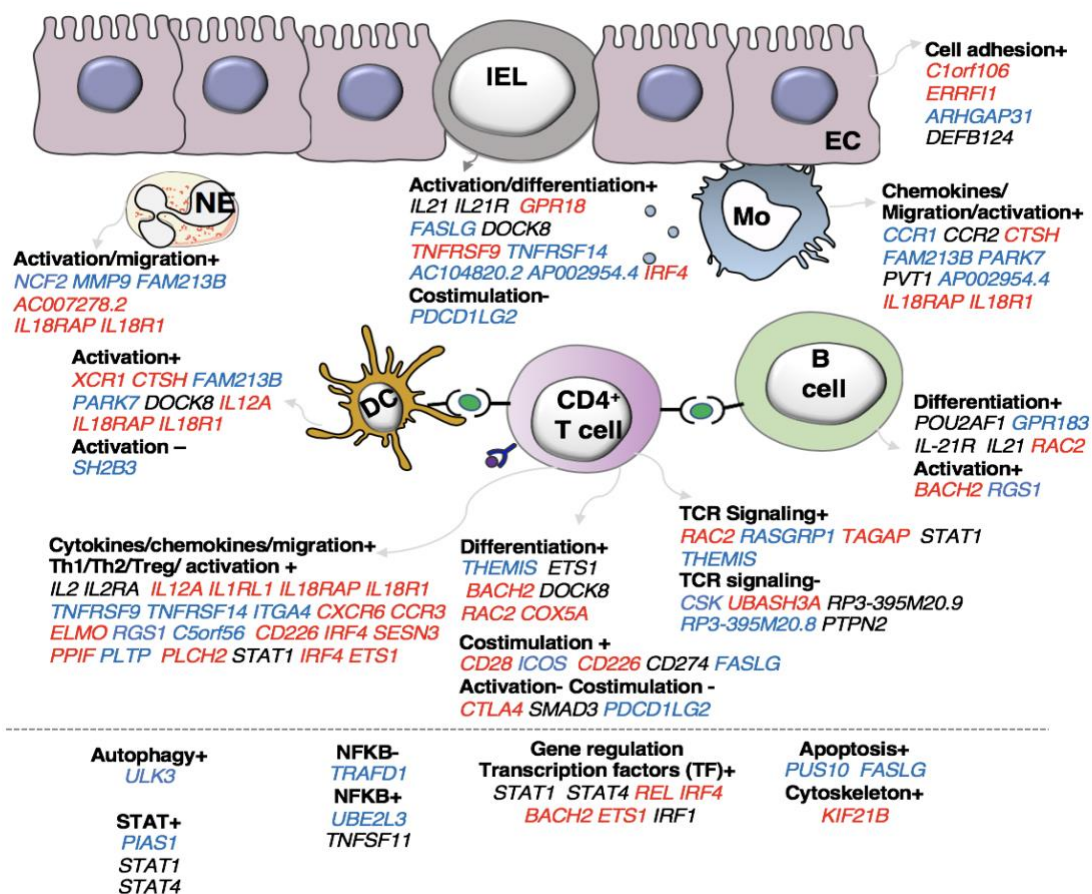
### 501 **CeD candidate genes operate in immune and intestinal epithelial cells**

502 To complement our REACTOME gene set enrichment analysis and dig deeper into the  
 503 biological processes and cell types in which the prioritized genes may act, we analysed their  
 504 expression profiles in available RNA-seq datasets from disease-relevant cell types including  
 505 1) small intestinal biopsies of active CeD patients and healthy controls, 2) intra-epithelial  
 506 cytotoxic lymphocytes (IE-CTLs) stimulated with disease-relevant cytokines IL-21, IL-15 and  
 507 IFN $\beta$ , and 3) gluten specific CD4+ T cells (gsCD4+ T cells) stimulated with antiCD3-antiCD28,  
 508 which mimics the disease-specific response to gluten peptides (**Fig. 2C**) (differentially  
 509 expressed genes for each dataset are available in **Supplementary Table 6**). We observed  
 510 that the genes grouped in co-regulation clusters 1 and 2 are highly expressed in small  
 511 intestinal biopsies and IE-CTLs, which is in line with the IFN $\gamma$  pathway enrichment seen in  
 512 co-regulation cluster 2 (**Fig. 2B**). IFN $\gamma$  is mainly produced by gsCD4+ T cells and IE-CTLs  
 513 and is known to disrupt the integrity of the intestinal epithelial cells in CeD-associated villous

514 atrophy<sup>52-54</sup>. Within this cluster we also found genes specific to antigen-presenting cells (B  
 515 cells, monocytes and dendritic cells) and epithelial cells such as *IL12A* and *COLCA1*, which  
 516 are most expressed in small intestinal biopsies (**Fig. 2C**). The genes in co-regulation  
 517 clusters 3 and 4 are highly expressed in gsCD4+T cells, especially after stimulation with  
 518 antiCD3-antiCD28, indicating that these prioritized genes may be biologically relevant in the  
 519 immediate T cell receptor response to gluten ingestion.

520 The gene expression pattern of the prioritized genes, when combined with  
 521 information from our literature search, suggests that these genes may control general  
 522 biological processes (e.g. apoptosis, gene regulation and cytoskeleton remodelling) as well  
 523 as specific immune functions (e.g. cell adhesion, cell differentiation and TCR signalling) in  
 524 diverse cell types (e.g. T cells, neutrophils, B cells, monocytes, epithelial cells) (**Fig. 3** and  
 525 **Supplementary Table 7**). The non-HLA genetic loci associated to CeD thus seem to affect  
 526 a complex network of cells and biological processes.

527



528

529 **Fig. 3 CeD candidate genes operate in immune cells and intestinal epithelial cells.**  
 530 Functions and cell types highlighted by the prioritized genes, according to our literature review  
 531 (see **Methods**) (n=118 genes, for 37 genes neither a function nor a specific cell type on which  
 532 the gene may operate could be specified). All genes contributing to a specific function are listed  
 533 under the sub-heading and coloured according to the change that leads to increased CeD risk:  
 534 increased expression (red), decreased expression (blue), or undefined (black). The symbols + or  
 535 - denote if a biological process is thought to be induced or repressed by the gene, respectively,  
 536 according to literature.

537 **Mediation analysis uncovers *TRAFD1* as a major *trans*-eQTL regulator**

538 To further understand the potential regulatory function of the prioritized genes, we identified  
539 downstream regulatory effects by performing a *trans*-mediation analysis using a two-step  
540 approach (**Methods**) (**Supplementary Fig. 1A**). We first considered all genes with a *trans*-  
541 eQTL ( $p < 5 \times 10^{-8}$ ) located in any of the 58 CeD-associated regions, then performed a  
542 mediation analysis by re-assessing the *trans*-eQTL effect after adjusting the expression  
543 levels for the expression of the prioritized gene(s) in the same locus (**Fig. 4A**).

544 Of the 497 possible prioritized gene–*trans*-eQTL gene combinations, we found 172  
545 that exhibited significant mediation effects. These combinations map to 13 associated  
546 regions and represent 21 unique mediating *cis*-eQTL genes and 79 unique mediated *trans*-  
547 eQTL genes (**Supplementary Table 8**). Among all the associated regions, the CeD-  
548 associated region on chromosome 12 contained the largest number of both *cis*-mediating  
549 genes (N=5) and *trans*-mediated genes (N=60). In this region, *TRAFD1* mediated more *trans*  
550 genes than all of the other regional *cis*-regulators and also had the highest mediation impact  
551 (average Z-score difference in effect size between mediated and unmediated analysis =  
552 2.79) (**Methods**) (**Supplementary Table 8**) (**Supplementary Fig. 1B**). Of note, the top  
553 eQTL variant of *TRAFD1* is a missense variant in the nearby gene *SH2B3*. This missense  
554 variant has been associated to a number of complex traits, including blood cell types and  
555 platelets, and autoimmune diseases<sup>55,56</sup>. However, we found that cell-type composition did  
556 not affect the eQTL-association of *TRAFD1* in our cohort ( $p > 0.044$  for 24 different cell-type  
557 traits) (**Methods**) (**Supplementary Table 9**). To ensure that the mediated *trans* genes of  
558 *TRAFD1* were not mediated by *SH2B3*, we corrected *TRAFD1* expression levels for *SH2B3*  
559 and re-ran the mediation analysis. Here we found that the mediating effect of *TRAFD1* was  
560 still significant for all 41 genes found initially and that the median Z-score difference between  
561 mediated and unmediated was higher than that of *SH2B3*, although it was slightly attenuated  
562 compared to the original *TRAFD1* signal (**Supplementary Table 10**) (**Supplementary**  
563 **Figure 1B**). Based on these results, we conclude that *TRAFD1* is a master regulator of gene  
564 expression changes in the associated region (**Fig. 4B**) (**Supplementary Table 10**).

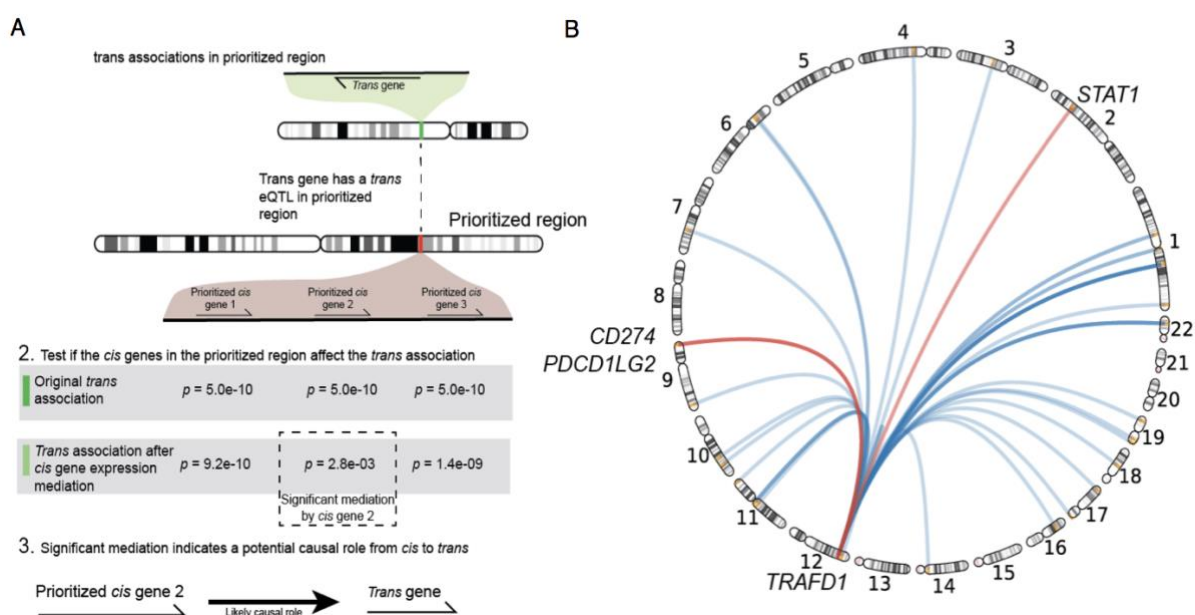
565 Strikingly, three of the *TRAFD1* *trans*-mediated genes – *STAT1*, *CD274* and  
566 *PDCD1LG2* – are also prioritized *cis*-genes in their respective loci (**Fig. 4B**). These results  
567 suggest that the *trans*-mediated *TRAFD1*-effects may have an additional additive effect in  
568 these CeD-associated loci.

569

570

571





572

573 **Fig. 4 Mediation analysis uncovers *TRAFD1* as a major *trans*-eQTL regulator.** (A) Workflow  
 574 illustrating the main steps to identify *trans*-eQTL genes mediated by our *cis*-prioritized genes.  
 575 First, we identified *trans*-eQTLs and *trans* genes that have a significant association ( $p < 5 \times 10^{-8}$ )  
 576 in our prioritized regions. Then, for every *cis* prioritized gene in the CeD-associated region, a  
 577 mediation analysis was performed to determine if the *cis* gene expression explains the *trans*-  
 578 eQTL effect. (B) Circular ideogram depicting the mediating effect of *TRAFD1* on 41 *trans* genes.  
 579 Three of the 41 *trans*-mediated genes were also prioritized by our *cis*-eQTL analysis (red).

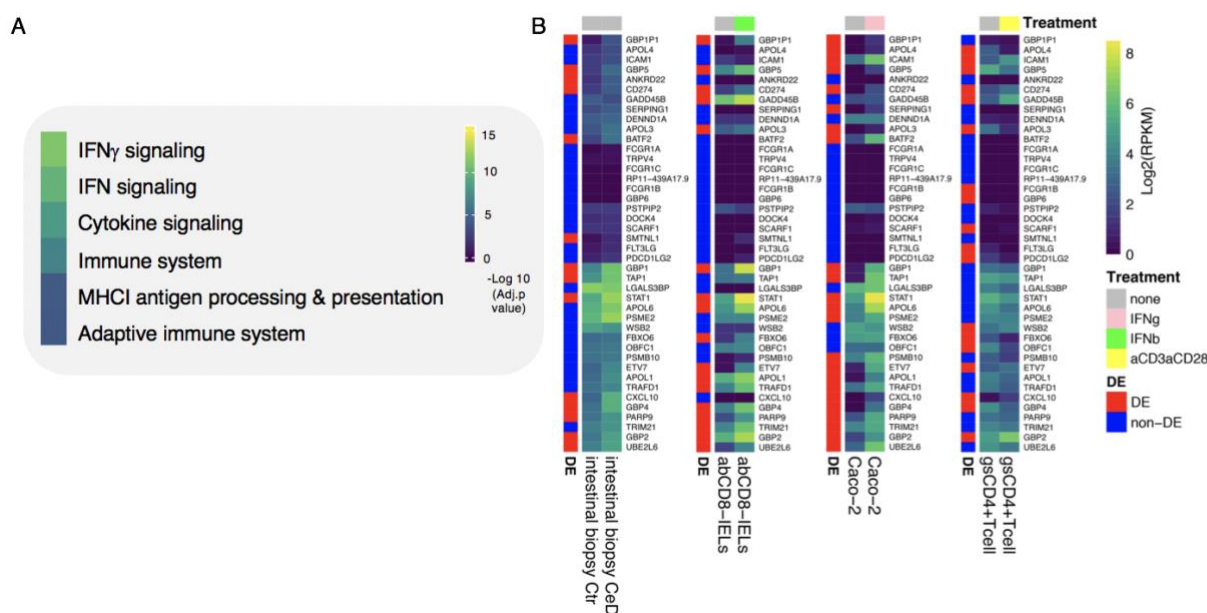
580

581 *TRAFD1* is a poorly characterized gene that has been suggested to act as a negative  
 582 regulator of the NF $\kappa$ B pathway<sup>57</sup>. To further elucidate the biological processes in which the  
 583 41 *TRAFD1* *trans*-mediated genes could be involved, we performed a REACTOME 2016  
 584 gene set enrichment analysis (**Supplementary Table 11**). Here we found that IFN $\gamma$   
 585 signalling, cytokine signalling and major histocompatibility complex class I (MHC I) antigen  
 586 processing / presentation are strongly enriched pathways, which points to a role for *TRAFD1*  
 587 and *TRAFD1* *trans*-mediated genes in antigen presentation and immune response (**Fig. 5A**).

588 By looking into RNA-seq datasets from disease-relevant cell types, we noted that  
 589 most *TRAFD1* *trans*-mediated genes are upregulated in biopsies from patients with active  
 590 CeD, and these genes include *STAT1*, *CXCL10* and *TAP1*, which are essential for IFN  
 591 response<sup>58</sup>, chemotaxis<sup>59</sup> and antigen processing<sup>60</sup>, respectively (**Fig. 5B**). Moreover, most  
 592 *TRAFD1* *trans*-mediated genes exhibit an increase in expression in response to IFN $\gamma$  in  
 593 intestinal epithelial cells (Caco-2) or IFN $\beta$  in IE-CTLs (**Fig. 5B**). In contrast, antiCD3-  
 594 antiCD28 stimulation in gsCD4<sup>+</sup>T cells resulted in both up- and downregulation of the  
 595 *TRAFD1* *trans*-mediated genes, implying that *TRAFD1* *trans*-mediated genes respond more  
 596 strongly to IFN signalling (IFN $\gamma$  or IFN $\beta$ ) than to TCR activation by anti-CD3/anti-CD28.

597 Indeed, the enrichment of the 41 *TRAFD1* trans-mediated genes in significantly differentially  
 598 expressed genes in biopsies, IE-CTLs, epithelial cells and gsCD4+Tcells was strongest in IE-  
 599 CTLs and epithelial cells upon IFN signalling (**Supplementary Table 6**). Overall, our results  
 600 suggest that *TRAFD1* and *TRAFD1* trans-mediated genes modulate IFN signalling upon  
 601 antigen presentation, possibly via regulation of NF $\kappa$ B, in CeD pathology.

602



603

604 **Fig. 5 *TRAFD1* is a regulator of IFN $\gamma$  signaling genes.** (A) Results of the REACTOME gene  
 605 set enrichment analysis of *TRAFD1*-mediated genes (n=41 genes). Colour code denotes the  
 606 significance (-log<sub>10</sub> adjusted *p* value) of each biological pathway. (B) Unscaled heatmaps  
 607 depicting the expression of these genes in RNA-seq datasets from different cell types: whole  
 608 biopsies from controls (Ctr, n=5 samples) of CeD patients (CeD, n=6 samples); intraepithelial  
 609 cytotoxic lymphocytes (IE-CTLs) unstimulated or treated with IFN $\beta$  for 3 hours (n=8 samples per  
 610 condition); and Caco-2 cells untreated or stimulated with IFN $\gamma$  for 3 hours (n=8 samples per  
 611 condition). Red indicates that a gene is differentially expressed (DE), blue indicates that a gene  
 612 is not differentially expressed (non-DE) (FDR<0.01 and |log<sub>2</sub>(RPKM)>1|). Grey (none or  
 613 unstimulated), pink (IFN $\gamma$ ), green (IFN $\beta$ ) and yellow (antiCD3/antiCD28) colours indicate the type  
 614 of stimulation (treatment).

615

### 616 ***TRAFD1* KD affects immune-activation genes**

617 We performed a siRNA KD experiment on *TRAFD1* to gain more insights into the biological  
 618 function of this gene and to independently validate the *TRAFD1* trans-mediated genes. We  
 619 also evaluated the transcriptional changes of knocking down *TRAFD1* in the monocyte-like  
 620 cell line THP-1 under resting conditions (unstimulated) or in the presence of LPS, a known  
 621 inducer of the NF $\kappa$ B pathway<sup>61</sup>.

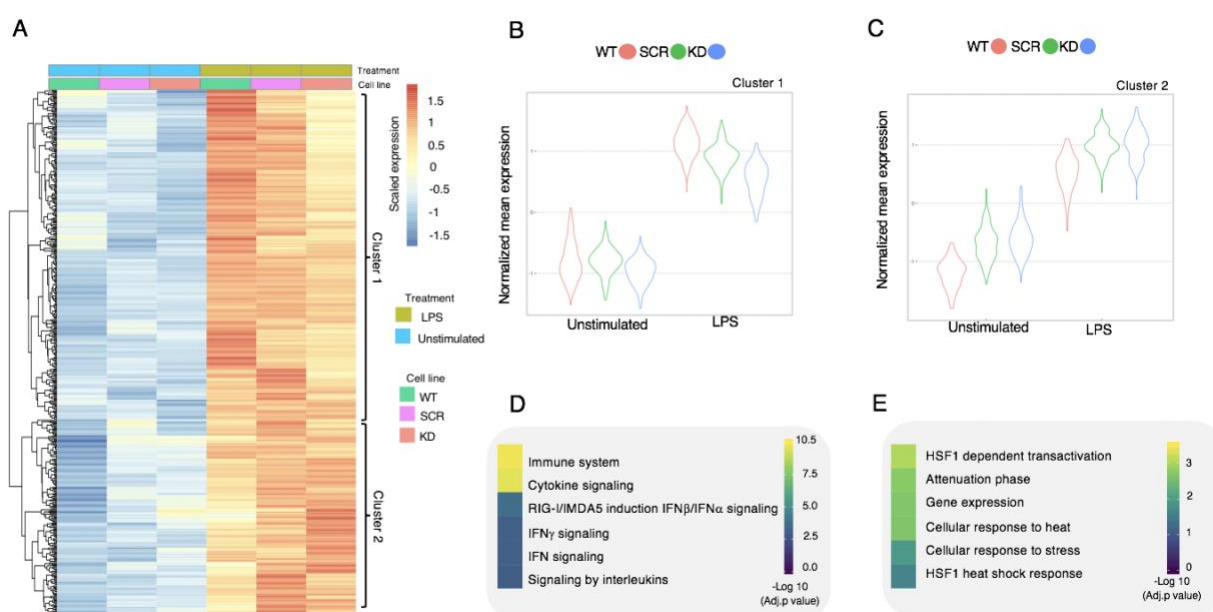
622 After siRNA treatment, we observed no significant differences in cell viability or  
623 proliferation among the controls (WT and SCR) and the KD treatment (**Supplementary Fig.**  
624 **2A, B**). However, as expected for the KD cell line, we noted a significant reduction in the  
625 expression of *TRAFD1* compared to the controls in WB and qPCR analyses  
626 (**Supplementary Fig. 2C-E**). KD of *TRAFD1* was also confirmed in the RNAseq data, with  
627 *TRAFD1* expression levels reduced by 41% in unstimulated KD cells compared to  
628 unstimulated SCR cells (adjusted  $p = 0.004$ ) and by 34% in LPS-stimulated KD cells  
629 compared to LPS-stimulated SCR cells (not significant) (**Supplementary Table 12**). The  
630 reduced KD effect upon LPS stimulation is consistent with our expectation that *TRAFD1* acts  
631 as negative regulator of the NF $\kappa$ B pathway, which is activated by several stimuli, including  
632 LPS<sub>61</sub>. Thus, the KD was successful and neither the transfection method nor a reduced  
633 expression of *TRAFD1* had a toxic effect (**Supplementary Fig. 2A-E**).

634 Next, we tested if the 41 *TRAFD1* *trans*-mediated genes were more differentially  
635 expressed than expected after LPS stimulation (**Supplementary Fig. 3**). To disentangle  
636 differential expression from the co-expression inherently present in a gene expression  
637 dataset, we devised a permutation scheme that compared the control (WT vs. SCR)  
638 observations with the KD (SCR vs. KD) observations (see **Methods**). This scheme takes  
639 into account the co-expression of a gene set, as this co-expression is present in both the  
640 control and the experimental observation. After performing 1,000,000 permutations of 42  
641 genes (41 *trans* mediated genes and *TRAFD1*) in the LPS-stimulated comparison, the  
642 median test statistic in the control observations was observed 54 times more often than in  
643 the KD observations (0.270% for WT-SCR vs. 0.005% for SCR-KD, **Supplementary Fig. 4**).  
644 This indicates that the 41 *trans*-mediated genes and *TRAFD1* are 54 times more  
645 differentially expressed than expected. We did not find increased differential expression of  
646 the same gene set in the unstimulated condition (1.120% for WT-SCR vs. 0.307% for SCR-  
647 KD, **Supplementary Fig. 4**), indicating that *TRAFD1* mainly regulates genes in an LPS-  
648 stimulated state.

649 To identify the role of *TRAFD1* in immune cells and processes, we compared gene  
650 expression changes in the unstimulated condition versus the LPS stimulated condition for  
651 each treatment (WT, SCR or KD) separately (**Supplementary Fig. 2F**). Differential  
652 expression analysis showed that 353 genes were uniquely upregulated and 330 genes  
653 uniquely downregulated after *TRAFD1* KD treatment (**Supplementary Fig. 2G, H**). We  
654 found no REACTOME gene set enrichment for these unique KD genes. We found 500  
655 upregulated and 433 downregulated genes that were differentially expressed in all three  
656 treatments upon LPS stimulation (**Fig. 6A, Supplementary Fig. 2G, H**). Upregulation (or  
657 downregulation) after LPS stimulation was treatment-dependent, i.e. the differential

658 expression identified was increased (or decreased) from WT to SCR to KD (**Fig. 6A**). We  
 659 performed hierarchical clustering, this separated the two gene sets into two clusters: cluster  
 660 1 shows a decreased response of genes in the *TRAFD1* KD group (LPS cluster 1, **Fig. 6B**,  
 661 **Supplementary Table 13**) and cluster 2 displays an increased expression in the *TRAFD1*  
 662 KD cells under unstimulated conditions that persists after LPS stimulation (LPS cluster 2,  
 663 **Fig. 6C**, **Supplementary Table 13**). REACTOME gene set enrichment analysis indicated  
 664 that the genes in LPS cluster 1 are involved in immune-related processes (e.g. cytokine  
 665 signalling, RIG/IMDA5 induction of IFN signalling and IFN signalling, **Fig. 6D**), whereas the  
 666 genes in LPS cluster 2 are associated with the heat shock response, which has been shown  
 667 to be activated as a consequence of immune activation or immune response to stress<sup>62</sup> (**Fig.**  
 668 **6E**, **Supplementary Table 13**). Together, these results suggest that *TRAFD1* is a regulator  
 669 of immune activation and inflammation.

670



671

672 **Fig 6. *TRAFD1* knockdown affects immune activation and stress-related genes. (A)**  
 673 **Heatmap showing the expression profile of the 500 shared DEGs identified in the knockdown**  
 674 **experiments (see **Methods** and **Supplementary Fig. 2 F, G**). A dendrogram on the left of the**  
 675 **heatmap depicts the strength of similarities based on Ward distance. (B, C) Violin plots showing**  
 676 **the normalized gene expression of the genes belonging to the first and second cluster of DEGs**  
 677 **identified in (A) in THP-1 cells under different experimental conditions (WT=untransfected,**  
 678 **SCR=non-targeting siRNA, KD=siRNA targeting *TRAFD1*) and stimulations**  
 679 **(LPS=lipopolysaccharide). (D, E) Results of REACTOME gene set enrichment analysis of the**  
 680 **genes within the first (D) and second cluster (E). Significance (-log<sub>10</sub> adjusted *p* value) of each**  
 681 **biological pathway is indicated by the colour key.**

682

683



## 684 Discussion

685 In the present study we aimed to identify CeD candidate genes using four *in silico* methods  
686 (MR-IVW, COLOC, LD overlap and DEPICT) and whole blood transcriptomics data from a  
687 population-based cohort. While previous studies have used at least one of these  
688 methods<sup>3,5,6,11</sup>, to our knowledge this is the first effort that integrates the four different  
689 statistical approaches. This systematic prioritization approach resulted in 118 prioritized  
690 causal genes, including 26 that are direct targets of an approved drug or of drugs under  
691 development for other complex diseases, including autoimmune diseases. The co-  
692 expression pattern within a large RNA-seq dataset from blood<sup>34</sup> suggests these genes are  
693 involved in cytokine signalling in innate and adaptive cells as well as in T cell activation  
694 pathways. We also identified *TRAFD1* to be *trans*-regulator of 41 genes, with a strong  
695 enrichment in IFN $\gamma$  signalling and MHC I antigen processing/presentation pathways, which  
696 are pivotal for the disease pathogenesis.

697 After clustering our *cis*-eQTL prioritized genes on shared co-regulation, we identified a  
698 cluster of genes involved in T cell activation and co-stimulation (cluster 3), highlighting a key  
699 role for T cell activation in the pathogenesis of CeD<sup>63</sup>. Within this co-regulation cluster we  
700 found the *THEMIS*, *IL2*, *CD28*, *CTLA4* and *UBASH3A* genes (**Fig. 2**), whose functions  
701 include T cell differentiation and activation and the TCR macromolecular complex.

702 Another co-regulation cluster (cluster 4, **Fig.2**) grouped prioritized genes involved in  
703 cytokine and chemokine signalling events that affect the microenvironment during  
704 inflammation in the intestinal mucosa. For example, this group included *CCR1* and *CCR2*,  
705 which control the activation and recruitment of inflammatory cells such as monocytes,  
706 dendritic cells and neutrophils<sup>64</sup>. *IL21* was also included in this co-regulation cluster. This  
707 gene encodes IL-21, providing proliferation and survival signals to B cells<sup>65</sup>, which in turn  
708 produce the autoantibodies detected in CeD and could act as antigen-presenting cells for  
709 g<sub>s</sub>T cells, thus enhancing the inflammatory response<sup>66</sup>. Next to chemokine receptors, this  
710 co-regulation cluster contains cytokine receptor genes, e.g. *IL18RAP* and *IL18R1*. Which  
711 encode the IL-18 receptor, that is expressed in intestinal epithelial cells and mediates IL-18  
712 controlled intestinal barrier integrity and immunity<sup>67,68</sup>. This cluster also contains transcription  
713 factors genes, e.g. *IRF4*, *ETS1* and *REL*. *IRF4* and *ETS1* are essential for T helper 1 (Th1)  
714 differentiation<sup>69,70</sup>. Interestingly, g<sub>s</sub>CD4<sup>+</sup> T cells exhibit a Th1 profile, that predominantly  
715 produce IFN $\gamma$ , a cytokine that affects the integrity of the intestinal epithelial cells contributing  
716 to villous atrophy<sup>52–54</sup>. *REL*, that is also contained in cluster 4, is a key regulator of NF $\kappa$ B  
717 signalling pathway, a major mediator of inflammation<sup>71</sup>, which is in line with the novel genetic  
718 association reported between NF $\kappa$ B and CeD by Ricano-Ponce et al.<sup>5</sup> Moreover, CeD

719 patients show a persistent activation of the NF $\kappa$ B pathway in the intestinal mucosa<sup>72</sup> as well  
720 as a significant increase in the methylation level of 8 genes that belong to this pathway<sup>73</sup>.  
721 Thus, these results indicate that CeD patients present with a major defect in the NF $\kappa$ B  
722 signalling complex.

723 For practical reasons, most prioritization studies have been focused on incorporating  
724 *cis*-eQTLs<sup>74</sup> and have mostly ignored *trans*-eQTLs, thus potentially missing long-distance  
725 co-regulated interactions<sup>74</sup>. In our study, we took advantage of a large transcriptomics cohort  
726 to run a *trans* mediation analysis for CeD loci. One of the most remarkable findings of this  
727 approach was that 41 *trans*-mediated genes were found to be controlled by a single gene:  
728 *TRAFD1*. These 41 genes are enriched for IFN $\gamma$  and MHC I antigen processing/presentation  
729 signalling pathways. Interestingly, gsCD4<sup>+</sup> T cells exhibit a Th1 profile and produce a large  
730 amount of IFN $\gamma$ , one of the most predominant cytokines in CeD<sup>54</sup>. Some of the most striking  
731 effects of IFN $\gamma$  include induction of apoptosis in intestinal epithelial cells, alteration of  
732 intestinal permeability and activation of monocytes and dendritic cells, which may act as  
733 antigen-presenting cells for gsCD4<sup>+</sup> T cells<sup>75</sup>.

734 *TRAFD1* is thought to be a regulator of the NF $\kappa$ B signalling pathway<sup>57</sup>, suggesting  
735 that CeD-risk SNPs may modulate the NF $\kappa$ B complex via both *cis* and *trans* regulatory  
736 mechanisms. Our results also point to a role for *TRAFD1* in response to IFN $\gamma$ ; however, IFN $\gamma$   
737 does not typically activate NF $\kappa$ B signaling<sup>76</sup> and the *IFNG* locus is not associated with CeD<sup>7</sup>.  
738 Thus, *TRAFD1* may activate the production of other cytokines, which in turn activate the  
739 NF $\kappa$ B complex.

740 IE-CTLs, which are the effector cells in CeD, have not thus far been genetically  
741 associated with the disease. However, given that MHC-I antigen presentation  
742 presentation/processing are essential for IEL activation and the striking activation of the 41  
743 *trans* mediated genes in IE-CTLs upon IFN stimulation, we propose that the IE-CTLs are  
744 also genetically linked to the disease through the action of *TRAFD1*.

745 Despite the approaches implemented in our study to uncover the novel gene  
746 interactions and biological pathways that may underlie the disease, a major drawback is the  
747 limited genome coverage of the CeD summary statistics used in this study. These were  
748 derived from a GWAS that used the Immunochip platform, a genotyping platform that only  
749 measures genotypes in regions known to be associated with immune function. We thus  
750 acknowledge that our current interpretation of CeD loci is biased toward immune-related  
751 mechanisms. Only when comprehensive whole-genome CeD association analyses have  
752 been performed will we have an unbiased understanding of the disease pathophysiology.

753           In our gene prioritization we observed that the different statistical gene prioritization  
754 methods applied to our data prioritized unique and jointly prioritized genes. Therefore, we  
755 recommend that investigators incorporate multiple methodologically orthogonal gene  
756 prioritization methods to identify a more comprehensive set of causal genes for a given  
757 disease. Here, we use two different (orthogonal) expression datasets (BIOS and DEPICT)  
758 and three prioritization methods using the same underlying data: MR-IVW, LD-overlap and  
759 COLOC. While we believe that the genes prioritized in this study represent robustly  
760 prioritized genes for CeD, it is difficult to validate if all the prioritized genes are truly causal  
761 based on statistical methodology alone. Functional validation of these genes in disease  
762 context is needed to rule out false positives.

763           The functional validation of *TRAFD1* in the siRNA KD experiment in THP-1 cells  
764 does establish that this gene regulates the *trans*-mediated network identified by our eQTL  
765 and statistical analysis. Still, the effects of the SCR control and the transfection itself may  
766 have obscured some specific *TRAFD1*-mediated effects. Moreover, the CeD-associated  
767 effects of *TRAFD1* may not be most pronounced in monocytes or upon LPS-stimulation.  
768 Indeed, context- and cell-type-specific effects of CeD-associated genetic variation may  
769 hamper the identification of the downstream effects of the prioritized *cis*- and *trans*-genes.

770           In conclusion, this study provides a framework for predicting candidate genes and  
771 their function using a systematic *in silico* approach that could be extended to other complex  
772 diseases. Using this approach, we not only confirmed previous association between  
773 adaptive cells (gsCD4+ T cells and B cells) and CeD, we also unveiled a link between  
774 specific genes that may contribute to the disease via innate immune cells, epithelial cells  
775 and IE-CTLs. Finally, we found a gene network controlled by *TRAFD1* that is part of two  
776 major pathways of immune activation, IFN $\gamma$  signalling and MHC I antigen processing.

777

778 **Acknowledgements.** We are very grateful for the altruistic donation of biological materials  
779 by the study participants, without them this study would not be possible. In addition, we  
780 thank the UMCG Genomics Coordination center, and the UG Center for Information  
781 Technology, and their sponsors BBMRI-NL & TarGet, for storage and computing  
782 infrastructure. We thank BBMRI-NL for providing the transcriptome and genotyped data for  
783 the BIOS cohort. We would like to thank Prof. Bana Jabri for providing IE-CTL cell lines,  
784 Prof. Morris Swertz for data storage and cluster facilities and Kate McIntyre for editing the  
785 manuscript. This work was supported by an ERC Advanced grant [FP/2007-2013/ERC grant  
786 2012-322698] and an NWO Spinoza prize grant [NWO SPI 92-266] to C.W. I.J is supported  
787 by a Rosalind Franklin Fellowship from the University of Groningen and an NWO VIDI grant  
788 [016.171.047].

789

#### 790 **Data Availability**

791 Summary statistics of the CeD GWAS are available from the European Genome-Phenome  
792 Archive (<https://www.ebi.ac.uk/ega/studies/EGAS00001003805>) under accession number  
793 EGAS00001003805. The individual-level data of the BIOS cohort is available upon request  
794 from <https://www.bbmri.nl/acquisition-use-analyze/bios>.

795

## 796 **Supplementary figure legends**

797 **Supplementary Fig. 1 Mediation effect on *trans* genes for all prioritized genes in the**  
798 ***TRAFD1* region on chromosome 12. (A)** Three boxes with the eQTL association curves of  
799 *TRAFD1*, *SERPING1* and *SERPING1* after mediation with *TRAFD1*. **(B)** Scatter plot indicating  
800 the absolute Z difference between unmediated and mediated *trans* associations upon mediation  
801 (y axis) by all mediating *cis* genes in the *TRAFD1* region shown on the x axis as well as when  
802 correcting *TRAFD1* expression for the expression of *SH2B3* ('*TRAFD1* – *SH2B3*').

803 **Supplementary Fig. 2 *TRAFD1* knockdown validation.** Cell viability **(A)** and proliferation **(B)** of  
804 THP-1 cells that were left untransfected (WT) or transfected with non-targeting siRNA (SCR) or  
805 siRNA targeting *TRAFD1* (KD) for 72 hours. Protein and mRNA levels of *TRAFD1* were  
806 determined by WB **(C, D)** and qPCR **(E)**. Bars indicate mean  $\pm$  SEM. Data are representative of  
807 three different experiments. Statistical differences were calculated with a one-sided t-test by  
808 using the SCR as 100% reference. p-value  $\leq$  0.0001 (\*\*\*\*). **(F)** The differential expression  
809 analysis approach. Here we compared the gene expression between unstimulated samples and  
810 their respective LPS-stimulated samples to identify DEGs that respond to stimulation ( $|\log_2$  FC)  
811  $>1$  and FDR  $\leq$  0.01). We then identified unique or shared DEGs responding to the stimulation  
812 between treatments (WT, SCR or KD), which are shown in two separate Venn diagrams: one for  
813 upregulated genes **(G)** and one for downregulated genes **(H)**.

814 **Supplementary Fig. 3 Expression pattern of *TRAFD1*-mediated genes upon *TRAFD1***  
815 **knockdown.** Heatmap showing the pattern of gene expression of *TRAFD1* and of the 41 genes  
816 it mediates, scaled by row (see details in **Methods** and **Fig. 5**). Expression is shown in different  
817 treatments and stimulations as indicated by coloured bars on top of the heatmap.

818 **Supplementary Fig. 4 DEGs upon *TRAFD1* knockdown are enriched in *TRAFD1*-mediated**  
819 **genes.** Here we compare the differential expression of 42 genes found in the *trans* mediation  
820 analysis of *TRAFD1* (41 *trans*-mediated genes and *TRAFD1*) with the differential expression of  
821 42 other randomly chosen genes. The histograms (blue) show the distribution of the median  
822 absolute T statistic of DEseq of 42 randomly chosen genes, when 1,000,000 sets of genes are  
823 randomly chosen, compared to the observed value for the 42 genes that are from the *trans*-  
824 mediation analysis (red horizontal line). We compare the results of the control experiment (WT-  
825 SCR) in panels **A** and **C** with the results of the knockdown experiment (SCR-KD) in panels **B** and  
826 **D**. The fold differences between the control experiments and the knockdown experiments show  
827 how much more than expected the 42 genes are differentially expressed in the knockdown  
828 compared to the control.

829

830

## 831 **Supplementary table Legends**

### 832 **Supplementary Table 1. Prioritization of genes likely causal for celiac disease (CeD).**

833 This table contains all the genes in the prioritized CeD regions and their evidence for being  
834 causal to CeD. One gene per row is shown. Columns (in order): the human build 37  
835 coordinates of the CeD region in which the gene is located (**region**); the gene name  
836 according to the ENSEMBL GENES 96 database (human build 37) (**gene\_name**); the  
837 ENSEMBL gene identifier (**ensembl\_id**); the most likely effect direction (determined as  
838 described in **Methods**) (**most\_likely\_direction**); number of independent eQTL variants  
839 found for the gene (**n\_eqtl\_effects**); the effect size (**MR\_ivw\_effect**) and *p* value  
840 (**MR\_ivw\_p\_value**) of the MR-IVW test; the summary of LD overlap  
841 (**ld\_overlap\_summary**), with either the top eQTL variant ('top\_snp') or an independent  
842 eQTL variant ('cojo\_snp') with the  $r_2$  linkage disequilibrium between the eQTL SNP and the  
843 CeD top variant; the coloc posterior probability of causal variants being shared (**coloc\_h4**); if  
844 the gene passes DEPICTs own false discovery thresholds (**depict\_fdr\_pass**); and the lines  
845 of evidence that are significant compared to the lines of evidence that are available for a  
846 gene (**lines\_of\_evidence**). Bold fields in any of the columns indicate that the prioritization  
847 method is significant according to our thresholds.

### 848 **Supplementary Table 2. Sensitivity analyses for genes selected by the IVW-MR**

849 **method.** In this table, genes with a significant MR-IVW effect are tested for heterogeneity  
850 using the Q test statistic and the MR-weighted median results as sensitivity analysis of all  
851 significant MR results. Each row contains the following information: the human build 37  
852 coordinates of the CeD region in which the gene is located (**region**); the gene name  
853 according to the ENSEMBL GENES 96 database (human build 37) (**gene\_name**); the  
854 ENSEMBL gene identifier (**ensembl\_id**); the most likely direction of the effect (determined  
855 as described in **Methods**) (**most\_likely\_direction**); the number of independent eQTL  
856 variants found (**n\_eqtl\_effects**); the effect size (**MR\_ivw\_effect**) and *p* value  
857 (**MR\_ivw\_p\_value**) of the MR-IVW test; the heterogeneity *p* value of the MR-IVW test using  
858 Cochran's Q statistic (**MR\_heterogeneity\_p\_value**); the weighted median effect estimate  
859 (**MR\_WM\_beta**) and its associated *p* value (**MR\_WM\_p**); the MR effect estimate after  
860 removal of potential outliers (**MR\_Q\_beta**); its associated *p* value (**MR\_Q\_p**); the remaining  
861 variants after outlier removal (**MR\_Q\_ivs**) and the heterogeneity estimate  
862 (**MR\_Q\_heterogeneity**).

### 863 **Supplementary Table 3. Druggability information for prioritized genes.**

864 This table contains all the prioritized *cis* genes in the CeD regions that are existing drug targets  
865 according to two different databases (DrugBank v5.1.4, and Finan et al.<sup>39</sup>). One gene per



866 row is shown. Columns indicate (in order): the human build 37 coordinates of the CeD region  
867 in which the gene is located (**region**); the gene name according to the ENSEMBL GENES  
868 96 database (human build 37) (**gene\_name**); the ENSEMBL gene identifier (**ensembl\_id**);  
869 the most likely effect direction (determined as described in **Methods**)  
870 (**most\_likely\_direction**); the number of independent eQTL variants found for the gene  
871 (**n\_eqtl\_effects**); the effect size (**MR\_ivw\_effect**) and  $p$  value (**MR\_ivw\_p\_value**) of the  
872 MR-IVW test; the summary of LD overlap (**ld\_overlap\_summary**) with either the top eQTL  
873 variant ('top\_snp') or an independent eQTL variant ('cojo\_snp') with the  $r_2$  linkage  
874 disequilibrium between the eQTL SNP and the CeD top variant; the coloc posterior  
875 probability of causal variants being shared (**coloc\_h4**); if the gene passes DEPICT's own  
876 false discovery thresholds (**depict\_fdr\_pass**); the lines of evidence that are significant  
877 compared to the lines of evidence that are available for a gene (**lines\_of\_evidence**); the  
878 druggability tier based on Finan et al.<sup>39</sup>, with lower tiers making it more likely that the gene is  
879 druggable<sup>39</sup>, (**druggable\_tier**), and if the gene is a drug bank drug target  
880 (**drug\_bank\_drug\_target**). Bold fields in any of the columns indicate that the prioritization  
881 method is significant according to our thresholds.

882 **Supplementary Table 4. Cluster assignments for the prioritized genes.** The 118  
883 prioritized genes were assigned to a cluster based on a guilt-by-association co-regulation  
884 approach to find shared biological mechanisms. For each gene that was prioritized  
885 (**ensembl\_id** and **gene\_name**), a cluster membership is given (**cluster\_membership**).

886 **Supplementary Table 5. Significant REACTOME 2016 enrichment of *cis* prioritized  
887 genes in each co-regulation cluster.** Results from the enrichr API using the gene clusters  
888 of **Supplementary Table 4** as query. Columns indicate: the enrichment background  
889 (**background**); the enrichment term in the background (**term\_name**); the non-corrected  $p$   
890 value of enrichment for this term (**p\_value**) and  $Z$  score (**Z\_score**); enrichr combined score  
891 (**combined\_score**); *cis*-prioritized genes found in each the term (**overlapping\_genes**) and  
892 the multiple testing corrected  $p$  value (**adjusted\_p\_value**). Each tab of the excel file contain  
893 the gene set enrichment for each cluster as defined in **Supplementary Table 4**.

894 **Supplementary Table 6. Results of DE analyses from all cell-type- and context-  
895 specific data available for this study (datasets).** This table lists all results for the DE  
896 analyses (Significant DE genes are defined as  $\text{padj} < 0.05$  and  $\log_2$  fold change  $> |1|$ ) and a  
897 summary report of the overlap with *TRAFD1* *trans*-mediated genes (**overlap with trans  
898 genes+TRAFD1**) and relative enrichment. The DE gene lists ( $\text{padj} < 0.05$  and  $\log_2$  fold  
899 change  $> |1|$ ) for each dataset are given in individual sheets. In the sheet "enrichment",  
900 columns upregulated and downregulated indicate if the *trans*-mediated genes are up- or



901 downregulated under stimulated conditions compared to control conditions in each dataset.  
902 Enrichment of all the trans mediated genes in the DE genes was determined using a  
903 Fisher's exact test and the enrichment  $p$  value is shown in the column enrichment p-val.

904 **Supplementary Table 7. Functions attributable to the prioritized genes, according to**  
905 **our literature review (see Methods and Fig. 3).** Columns describe (in order): gene name  
906 (**gene\_name**); ensemble ID (**ensembl\_id**); the change that leads to increased CeD risk, i.e.  
907 increased expression (+), decreased expression (-), or undefined (?) (**direction**); attributable  
908 function based in literature (**potential\_function**); and literature or web-based sources  
909 (**source\_1** and **source\_2**). Web-based sources include Gene cards  
910 (<https://www.genecards.org/>) and Genenetwork (<https://www.genenetwork.nl/>).

911 **Supplementary Table 8. All the significant *trans*-mediated genes from our *cis***  
912 **prioritization.** Each row contains a *cis*–*trans* gene pair described with both the ensembl id  
913 and hgnc gene name (**cis\_ensembl\_id**), (**cis\_gene\_name**), (**trans\_ensembl\_id**) and  
914 (**trans\_gene\_name**). Mediation effect and significance are shown using the Z score of the  
915 unmediated versus the mediated estimate (using the original unmediated standard error)  
916 (**z\_score\_difference**) and the mediation  $p$  value of the test defined by Friedman and  
917 Schatzkin (**mediation\_p**).

918 **Supplementary Table 9. Cell type mediation analysis.** We calculated to what extent cell  
919 types counted in the BIOS cohort affect the most highly associated *TRAFD1* eQTL variant.  
920 Columns show (in order): the specific cell type measurements or mediator (**mediator**); the  
921 effect size after mediation by the cell type (**mediated\_beta**); the original effect size  
922 (**unmediated\_beta**); difference in effect sizes between mediated and unmediated  
923 (**beta\_difference**); the standard error mediation effect size (**se**); the t-statistic of the beta  
924 differences (**t\_statistic**); a  $p$  value of the Friedman and Schatzkin test statistic (**p\_value**);  
925 the Pearson correlation coefficient between *TRAFD1* and the cell type proportion  
926 (**correlation**); and the number of observations in the BIOS cohort (**n\_observations**). If a  
927 mediator has a “\_Perc” suffix, the cell type counts were converted into ratios. Cell type  
928 abbreviations: Baso: Basophil count, EOS: eosinophil count, HCT: haematocrit, HGB:  
929 haemoglobin, LUC: large unstained cell count, Lymph: lymphocyte count, MCH: mean  
930 corpuscular haemoglobin, MCHC: mean corpuscular haemoglobin concentration, MCV:  
931 mean corpuscular volume, Mono: Monocyte count, MPV: mean platelet volume, Neut:  
932 Neutrophil count, PLT: platelets count, RBC: red blood cell count, RDW: red blood cell  
933 distribution width, WBC: white blood cell count.

934 **Supplementary Table 10. Mediation results when correcting *TRAFD1* expression for**  
935 **the nearby *SH2B3* expression.** Columns are: the ENSEMBL id (**ensemble\_id**); the hgnc  
936 gene name (**gene\_name**); and the mediation Z score difference (**Z\_score\_difference**), *p*  
937 value (**p\_value**) and Pearson correlation (**correlation**) between the *trans*-eQTL top variant  
938 and the residual of *TRAFD1* expression, after correction for *SH2B3* expression.

939

940 **Supplementary Table 11. Significant REACTOME 2016 enrichment of *TRAFD1*-**  
941 **mediated genes.** Results from the enrichr API using the mediated *TRAFD1 trans* genes as  
942 query. Columns indicate: the enrichment background (**background**); the enrichment term in  
943 the background (**term\_name**); the non-corrected *p* value of enrichment for this term  
944 (**p\_value**) and Z score (**Z\_score**); enrichr combined score (**combined\_score**); *cis*-  
945 prioritized genes found in each the term (**overlapping\_genes**) and the multiple-testing-  
946 corrected *p* value (**adjusted\_p\_value**).

947 **Supplementary Table 12. Differential expression results of the THP-1 experiments.**  
948 This table shows differential expression analysis of the THP-1 cells with 3 hr LPS treatment  
949 (LPS) or without LPS (Unstim) in wild type (WT), scrambled control siRNA (SCR) or  
950 *TRAFD1* knock down conditions (KD). All conditions and treatments were performed in  
951 triplicate. Complete DESEQ2 results are shown for each possible comparison in each tab.  
952 For each gene the columns show: the ensembl id per gene (**ensembl\_id**); the mean  
953 corrected expression of the gene (**baseMean**); the log2 fold change of the comparison  
954 (**log2FoldChange**); the standard error of this log2 fold change (**lfcSE**); a t-statistic of the  
955 log2foldchange (**stat**); the *p* value (**pvalue**); and the multiple testing adjusted *p* value (**padj**).  
956 The direction of the effect is always towards the second term in the tab name: if a log2 fold  
957 change is positive and the tab name is, for example, 'WT\_LPS\_vs\_SCR\_LPS', then the  
958 expression of the gene is increased in the SCR\_LPS samples compared to the WT\_LPS  
959 samples.

960 **Supplementary Table 13. Significant REACTOME 2016 enrichments in genes cells that**  
961 **are significantly upregulated by LPS in all treatments (WT, SCR and KD).** Reactome  
962 enrichment is shown for genes according in two groups: genes relatively downregulated in  
963 the *TRAFD1* knockdown experiment (REACTOME\_enrichment\_cluster1) and genes  
964 relatively upregulated in the *TRAFD1* knockdown experiment  
965 (REACTOME\_enrichment\_cluster2). Results are shown from the enrichr API analysis using  
966 the genes in a cluster as query. Columns indicate: the enrichment background  
967 (**background**); the enrichment term in the background (**term\_name**); the non-corrected *p*

968 value of enrichment for this term (**p\_value**) and Z score (**Z-score**); enrichr combined score  
969 (**combined\_score**); *cis*-prioritized genes found in each the term (**overlapping\_genes**) and  
970 the multiple testing corrected *p* value (**adjusted\_p\_value**).

971

## 972 **References**

- 973 1 Kuja-Halkola R, Lebwohl B, Halfvarson J, Wijmenga C, Magnusson PKE, Ludvigsson  
974 JF. Heritability of non-HLA genetics in coeliac disease: A population-based study in  
975 107 000 twins. *Gut* 2016. doi:10.1136/gutjnl-2016-311713.
- 976 2 Bevan S, Popat S, Braegger CP, Busch A, O'Donoghue D, Falth-Magnusson K *et al.*  
977 Contribution of the MHC region to the familial risk of coeliac disease. *J Med Genet*  
978 1999; **36**: 687–690.
- 979 3 Trynka G, Hunt KA, Bockett NA, Romanos J, Mistry V, Szperl A *et al.* Dense  
980 genotyping identifies and localizes multiple common and rare variant association  
981 signals in celiac disease. *Nat Genet* 2011; **43**: 1193–1201.
- 982 4 Dubois PCA, Trynka G, Franke L, Hunt KA, Romanos J, Curtotti A *et al.* Multiple  
983 common variants for celiac disease influencing immune gene expression. *Nat Genet*  
984 2010; **42**: 295–302.
- 985 5 Ricaño-Ponce I, Gutierrez-Achury J, Costa AF, Deelen P, Kurilshikov A, Zorro MM *et al.*  
986 Immunochip meta-analysis in European and Argentinian populations identifies two  
987 novel genetic loci associated with celiac disease. *Eur J Hum Genet* 2019; : 1–11.
- 988 6 Withoff S, Li Y, Jonkers I, Wijmenga C. Understanding Celiac Disease by Genomics.  
989 2016.
- 990 7 Kumar V, Gutierrez-Achury J, Kanduri K, Almeida R, Hrdlickova B, Zhernakova D V.  
991 *et al.* Systematic annotation of celiac disease loci refines pathological pathways and  
992 suggests a genetic explanation for increased interferon-gamma levels. *Hum Mol*  
993 *Genet* 2015; **24**: 397–409.
- 994 8 Ricaño-Ponce I, Zhernakova D V., Deelen P, Luo O, Li X, Isaacs A *et al.* Refined  
995 mapping of autoimmune disease associated genetic variants with gene expression  
996 suggests an important role for non-coding RNAs. *J Autoimmun* 2016; **68**: 62–74.
- 997 9 Zhernakova A, Stahl EA, Trynka G, Raychaudhuri S, Festen EA, Franke L *et al.* Meta-  
998 analysis of genome-wide association studies in celiac disease and rheumatoid  
999 arthritis identifies fourteen non-HLA shared loci. *PLoS Genet* 2011; **7**.  
1000 doi:10.1371/journal.pgen.1002004.
- 1001 10 Jonkers IH, Wijmenga C. Context-specific effects of genetic variants associated with  
1002 autoimmune disease. *Hum. Mol. Genet.* 2017. doi:10.1093/hmg/ddx254.
- 1003 11 Fernandez-Jimenez N, Bilbao JR. Mendelian randomization analysis of celiac GWAS  
1004 reveals a blood expression signature with diagnostic potential in absence of gluten  
1005 consumption. *Hum Mol Genet* 2019. doi:10.1093/hmg/ddz113.

- 1006 12 Giambartolomei C, Vukcevic D, Schadt EE, Franke L, Hingorani AD, Wallace C *et al.*  
1007 Bayesian Test for Colocalisation between Pairs of Genetic Association Studies Using  
1008 Summary Statistics. *PLoS Genet* 2014; **10**: e1004383.
- 1009 13 Burgess S, Butterworth A, Thompson SG. Mendelian randomization analysis with  
1010 multiple genetic variants using summarized data. *Genet Epidemiol* 2013; **37**: 658–  
1011 665.
- 1012 14 Graaf A van der, Claringbould A, Rimbert A, consortium B, Westra H-J, Li Y *et al.* A  
1013 novel Mendelian randomization method identifies causal relationships between gene  
1014 expression and low-density lipoprotein cholesterol levels. *bioRxiv* 2019; : 671537.
- 1015 15 Pers TH, Karjalainen JM, Chan Y, Westra HJ, Wood AR, Yang J *et al.* Biological  
1016 interpretation of genome-wide association studies using predicted gene functions. *Nat*  
1017 *Commun* 2015; **6**: 5890.
- 1018 16 Zhernakova D V., Deelen P, Vermaat M, Van Iterson M, Van Galen M, Arindrarto W *et*  
1019 *al.* Identification of context-dependent expression quantitative trait loci in whole blood.  
1020 *Nat Genet* 2017; **49**: 139–145.
- 1021 17 van Greevenbroek MMJ, Jacobs M, van der Kallen CJH, Vermeulen VMMJ, Jansen  
1022 EHJM, Schalkwijk CG *et al.* The cross-sectional association between insulin  
1023 resistance and circulating complement C3 is partly explained by plasma alanine  
1024 aminotransferase, independent of central obesity and general inflammation (the  
1025 CODAM study). *Eur J Clin Invest* 2011; **41**: 372–379.
- 1026 18 Deelen J, van den Akker EB, Trompet S, van Heemst D, Mooijaart SP, Slagboom PE  
1027 *et al.* Employing biomarkers of healthy ageing for leveraging genetic studies into  
1028 human longevity. *Exp Gerontol* 2016; **82**: 166–174.
- 1029 19 Tigchelaar EF, Zhernakova A, Dekens JAM, Hermes G, Baranska A, Mujagic Z *et al.*  
1030 Cohort profile: LifeLines DEEP, a prospective, general population cohort study in the  
1031 northern Netherlands: Study design and baseline characteristics. *BMJ Open* 2015; **5**:  
1032 e006772.
- 1033 20 Lin BD, Willemsen G, Abdellaoui A, Bartels M, Ehli EA, Davies GE *et al.* The Genetic  
1034 Overlap between Hair and Eye Color. *Twin Res Hum Genet* 2016; **19**: 595–599.
- 1035 21 Huisman MHB, De Jong SW, Van Doormaal PTC, Weinreich SS, Schelhaas HJ, Van  
1036 Der Kooi AJ *et al.* Population based epidemiology of amyotrophic lateral sclerosis  
1037 using capture-recapture methodology. *J Neurol Neurosurg Psychiatry* 2011; **82**:  
1038 1165–1170.
- 1039 22 Hofman A, Brusselle GGO, Murad SD, van Duijn CM, Franco OH, Goedegebure A *et*



- 1040 *al.* The Rotterdam Study: 2016 objectives and design update. *Eur J Epidemiol* 2015;  
1041 **30**: 661–708.
- 1042 23 Vösa U, Claringbould A, Westra H-J, Bonder MJ, Deelen P, Zeng B *et al.* Unraveling  
1043 the polygenic architecture of complex traits using blood eQTL metaanalysis. *bioRxiv*  
1044 2018; **18**: 447367.
- 1045 24 Das S, Forer L, Schönherr S, Sidore C, Locke AE, Kwong A *et al.* Next-generation  
1046 genotype imputation service and methods. *Nat Genet* 2016; **48**: 1284–1287.
- 1047 25 Chang CC, Chow CC, Tellier LCAM, Vattikuti S, Purcell SM, Lee JJ. Second-  
1048 generation PLINK: Rising to the challenge of larger and richer datasets. *Gigascience*  
1049 2015; **4**: 7.
- 1050 26 Dobin A, Davis CA, Schlesinger F, Drenkow J, Zaleski C, Jha S *et al.* STAR: Ultrafast  
1051 universal RNA-seq aligner. *Bioinformatics* 2013; **29**: 15–21.
- 1052 27 Boomsma DI, Wijmenga C, Slagboom EP, Swertz MA, Karssen LC, Abdellaoui A *et*  
1053 *al.* The Genome of the Netherlands: Design, and project goals. *Eur J Hum Genet*  
1054 2014; **22**: 221–227.
- 1055 28 Anders S, Pyl PT, Huber W. HTSeq-A Python framework to work with high-throughput  
1056 sequencing data. *Bioinformatics* 2015; **31**: 166–169.
- 1057 29 Yang J, Lee SH, Goddard ME, Visscher PM. GCTA: A tool for genome-wide complex  
1058 trait analysis. *Am J Hum Genet* 2011; **88**: 76–82.
- 1059 30 Auton A, Abecasis GR, Altshuler DM, Durbin RM, Bentley DR, Chakravarti A *et al.* A  
1060 global reference for human genetic variation. *Nature* 2015; **526**: 68–74.
- 1061 31 Burgess S, Thompson SG. Interpreting findings from Mendelian randomization using  
1062 the MR-Egger method. *Eur J Epidemiol* 2017; **32**: 377–389.
- 1063 32 Yang J, Ferreira T, Morris AP, Medland SE, Madden PAF, Heath AC *et al.* Conditional  
1064 and joint multiple-SNP analysis of GWAS summary statistics identifies additional  
1065 variants influencing complex traits. *Nat Genet* 2012; **44**: 369–375.
- 1066 33 Bowden J, Hemani G, Davey Smith G. Invited Commentary: Detecting Individual and  
1067 Global Horizontal Pleiotropy in Mendelian Randomization—A Job for the Humble  
1068 Heterogeneity Statistic? *Am J Epidemiol* 2018; **187**: 2681–2685.
- 1069 34 Deelen P, van Dam S, Herkert JC, Karjalainen JM, Brugge H, Abbott KM *et al.*  
1070 Improving the diagnostic yield of exome- sequencing by predicting gene–phenotype  
1071 associations using large-scale gene expression analysis. *Nat Commun* 2019; **10**.  
1072 doi:10.1038/s41467-019-10649-4.

- 1073 35 Freedman LS, Schatzkin A. Sample size for studying intermediate endpoints within  
1074 intervention trials or observational studies. *Am J Epidemiol* 1992; **136**: 1148–1159.
- 1075 36 Chen EY, Tan CM, Kou Y, Duan Q, Wang Z, Meirelles GV *et al.* Enrichr: interactive  
1076 and collaborative HTML5 gene list enrichment analysis tool. *BMC Bioinformatics*  
1077 2013; **14**: 128.
- 1078 37 Wishart DS, Feunang YD, Guo AC, Lo EJ, Marcu A, Grant JR *et al.* DrugBank 5.0: A  
1079 major update to the DrugBank database for 2018. *Nucleic Acids Res* 2018; **46**:  
1080 D1074–D1082.
- 1081 38 Whirl-Carrillo M, McDonagh EM, Hebert JM, Gong L, Sangkuhl K, Thorn CF *et al.*  
1082 Pharmacogenomics knowledge for personalized medicine. *Clin Pharmacol Ther* 2012;  
1083 **92**: 414–417.
- 1084 39 Finan C, Gaulton A, Kruger FA, Lumbers RT, Shah T, Engmann J *et al.* The  
1085 druggable genome and support for target identification and validation in drug  
1086 development. *Sci Transl Med* 2017; **9**: eaag1166.
- 1087 40 Kim D, Langmead B, Salzberg SL. HISAT: a fast spliced aligner with low memory  
1088 requirements. *Nat Methods* 2015; **12**: 357.
- 1089 41 Li H, Handsaker B, Wysoker A, Fennell T, Ruan J, Homer N *et al.* The Sequence  
1090 Alignment/Map format and SAMtools. *Bioinformatics* 2009; **25**: 2078–2079.
- 1091 42 Liao Y, Smyth GK, Shi W. The R package Rsubread is easier, faster, cheaper and  
1092 better for alignment and quantification of RNA sequencing reads. *Nucleic Acids Res*  
1093 2019. doi:10.1093/nar/gkz114.
- 1094 43 Anders S, Huber W. Differential expression analysis for sequence count data.  
1095 *Genome Biol* 2010; **11**: R106.
- 1096 44 Zorro MM, Aguirre-Gamboa R, Mayassi T, Ciszewski C, Barisani D, Hu S *et al.* Tissue  
1097 alarmins and adaptive cytokine induce dynamic and distinct transcriptional responses  
1098 in tissue-resident intraepithelial cytotoxic T lymphocytes. *J Autoimmun* 2020; **108**:  
1099 102422.
- 1100 45 Jabri B, De Serre NPM, Cellier C, Evans K, Gache C, Carvalho C *et al.* Selective  
1101 expansion of intraepithelial lymphocytes expressing the HLA-E- specific natural killer  
1102 receptor CD94 in celiac disease. *Gastroenterology* 2000; **118**: 867–879.
- 1103 46 Petersen J, Montserrat V, Mujico JR, Loh KL, Beringer DX, Van Lummel M *et al.* T-  
1104 cell receptor recognition of HLA-DQ2-gliadin complexes associated with celiac  
1105 disease. *Nat Struct Mol Biol* 2014; **21**: 480–488.

- 1106 47 Chiu YG, Ritchlin CT. Denosumab: targeting the RANKL pathway to treat rheumatoid  
1107 arthritis. *Expert Opin Biol Ther* 2017; **17**: 119–128.
- 1108 48 Lynch JP, Metz DC, Rutgeerts P, Vermeire S, Assche G Van. Biological Therapies for  
1109 Inflammatory Bowel Diseases. *Gastroenterology* 2009; **136**: 1182–1197.
- 1110 49 Baldassari LE, Rose JW. Daclizumab: Development, Clinical Trials, and Practical  
1111 Aspects of Use in Multiple Sclerosis. *Neurotherapeutics* 2017; **14**: 842–858.
- 1112 50 Goruppi S, Procopio MG, Jo S, Clocchiatti A, Neel V, Dotto GP. The ULK3 Kinase Is  
1113 Critical for Convergent Control of Cancer-Associated Fibroblast Activation by CSL and  
1114 GLI. *Cell Rep* 2017; **20**: 2468–2479.
- 1115 51 Vang T, Abrahamsen H, Myklebust S, Enserink J, Prydz H, Mustelin T *et al.*  
1116 Knockdown of C-terminal Src kinase by siRNA-mediated RNA interference augments  
1117 T cell receptor signaling in mature T cells. *Eur J Immunol* 2004; **34**: 2191–2199.
- 1118 52 Abadie V, Discepolo V, Jabri B. Intraepithelial lymphocytes in celiac disease  
1119 immunopathology. *Semin Immunopathol* 2012. doi:10.1007/s00281-012-0316-x.
- 1120 53 Nilsen EM, Lundin KEA, Krajci P, Scott H, Sollid LM, Brandtzaeg P. Gluten specific,  
1121 HLA-DQ restricted T cells from coeliac mucosa produce cytokines with Th1 or Th0  
1122 profile dominated by interferon  $\gamma$ . *Gut* 1995; **37**: 766–776.
- 1123 54 Wapenaar MC, Van Belzen MJ, Fransen JH, Fariña Sarasqueta A, Houwen RHJ,  
1124 Meijer JWR *et al.* The interferon gamma gene in celiac disease: Augmented  
1125 expression correlates with tissue damage but no evidence for genetic susceptibility. *J*  
1126 *Autoimmun* 2004; **23**: 183–190.
- 1127 55 Westra H-J, Martínez-Bonet M, Onengut-Gumuscu S, Lee A, Luo Y, Teslovich N *et al.*  
1128 Fine-mapping and functional studies highlight potential causal variants for rheumatoid  
1129 arthritis and type 1 diabetes. *Nat Genet* 2018; **50**: 1366–1374.
- 1130 56 Astle WJ, Elding H, Jiang T, Allen D, Ruklisa D, Mann AL *et al.* The Allelic Landscape  
1131 of Human Blood Cell Trait Variation and Links to Common Complex Disease. *Cell*  
1132 2016; **167**: 1415-1429.e19.
- 1133 57 Sanada T, Takaesu G, Mashima R, Yoshida R, Kobayashi T, Yoshimura A. FLN29  
1134 deficiency reveals its negative regulatory role in the toll-like receptor (TLR) and  
1135 retinoic acid-inducible gene I (RIG-I)-like helicase signaling pathway. *J Biol Chem*  
1136 2008; **283**: 33858–33864.
- 1137 58 Kim HS, Kim DC, Kim HM, Kwon HJ, Kwon SJ, Kang SJ *et al.* STAT1 deficiency  
1138 redirects IFN signalling toward suppression of TLR response through a feedback  
1139 activation of STAT3. *Sci Rep* 2015; **5**. doi:10.1038/srep13414.

- 1140 59 Majumder S, Bhattacharjee S, Paul Chowdhury B, Majumdar S. CXCL10 Is Critical for  
1141 the Generation of Protective CD8 T Cell Response Induced by Antigen Pulsed CpG-  
1142 ODN Activated Dendritic Cells. *PLoS One* 2012; **7**.  
1143 doi:10.1371/journal.pone.0048727.
- 1144 60 Seyffer F, Tampé R. ABC transporters in adaptive immunity. *Biochim. Biophys. Acta -*  
1145 *Gen. Subj.* 2015; **1850**: 449–460.
- 1146 61 Dorrington MG, Fraser IDC. NF- $\kappa$ B signaling in macrophages: Dynamics, crosstalk,  
1147 and signal integration. *Front Immunol* 2019; **10**: 705.
- 1148 62 Tsan M-F, Gao B. Heat shock proteins and immune system. *J Leukoc Biol* 2009.  
1149 doi:10.1189/jlb.0109005.
- 1150 63 Tye-Din JA, Galipeau HJ, Agardh D. Celiac disease: A review of current concepts in  
1151 pathogenesis, prevention, and novel therapies. *Front Pediatr* 2018.  
1152 doi:10.3389/fped.2018.00350.
- 1153 64 Esche C, Stellato C, Beck LA. Chemokines: Key players in innate and adaptive  
1154 immunity. *J Invest Dermatol* 2005; **125**: 615–628.
- 1155 65 Linterman MA, Beaton L, Yu D, Ramiscal RR, Srivastava M, Hogan JJ *et al.* IL-21  
1156 acts directly on B cells to regulate Bcl-6 expression and germinal center responses. *J*  
1157 *Exp Med* 2010. doi:10.1084/jem.20091738.
- 1158 66 Høydahl LS, Richter L, Frick R, Snir O, Gunnarsen KS, Landsverk OJB *et al.* Plasma  
1159 Cells Are the Most Abundant Gluten Peptide MHC-expressing Cells in Inflamed  
1160 Intestinal Tissues From Patients With Celiac Disease. *Gastroenterology* 2019.  
1161 doi:10.1053/j.gastro.2018.12.013.
- 1162 67 Jarret A, Jackson R, Duizer C, Healy ME, Zhao J, Rone JM *et al.* Enteric Nervous  
1163 System-Derived IL-18 Orchestrates Mucosal Barrier Immunity. *Cell* 2020.  
1164 doi:10.1016/j.cell.2019.12.016.
- 1165 68 Nowarski R, Jackson R, Gagliani N, De Zoete MR, Palm NW, Bailis W *et al.* Epithelial  
1166 IL-18 Equilibrium Controls Barrier Function in Colitis. *Cell* 2015.  
1167 doi:10.1016/j.cell.2015.10.072.
- 1168 69 Mahnke J, Schumacher V, Ahrens S, Käding N, Feldhoff LM, Huber M *et al.* Interferon  
1169 Regulatory Factor 4 controls T H1 cell effector function and metabolism. *Sci Rep*  
1170 2016; **6**: 35521.
- 1171 70 Grenningloh R, Bok YK, Ho IC. Ets-1, a functional cofactor of T-bet, is essential for  
1172 Th1 inflammatory responses. *J Exp Med* 2005; **201**: 615–626.

- 1173 71 Liu T, Zhang L, Joo D, Sun SC. NF- $\kappa$ B signaling in inflammation. *Signal Transduct.*  
1174 *Target. Ther.* 2017. doi:10.1038/sigtrans.2017.23.
- 1175 72 Maiuri MC, De Stefano D, Mele G, Fecarotta S, Greco L, Troncone R *et al.* Nuclear  
1176 factor  $\kappa$ B is activated in small intestinal mucosa of celiac patients. *J Mol Med* 2003;  
1177 **81**: 373–379.
- 1178 73 Fernandez-jimenez N, Castellanos-rubio A, Plaza-izurieta L, Irastorza I,  
1179 Elcoroaristizabal X, Jauregi-miguel A *et al.* Coregulation and modulation of NF $\kappa$ B-  
1180 related genes in celiac disease: Uncovered aspects of gut mucosal inflammation.  
1181 *Hum Mol Genet* 2014; **23**: 1298–1310.
- 1182 74 Brynedal B, Choi JM, Raj T, Bjornson R, Stranger BE, Neale BM *et al.* Large-Scale  
1183 trans-eQTLs Affect Hundreds of Transcripts and Mediate Patterns of Transcriptional  
1184 Co-regulation. *Am J Hum Genet* 2017; **100**: 581–591.
- 1185 75 Beitnes ACR, Ráki M, Brottveit M, Lundin KEA, Jahnsen FL, Sollid LM. Rapid  
1186 accumulation of CD14 +CD11c + dendritic cells in gut mucosa of celiac disease after  
1187 in vivo gluten challenge. *PLoS One* 2012. doi:10.1371/journal.pone.0033556.
- 1188 76 Deb A, Haque SJ, Mogensen T, Silverman RH, Williams BRG. RNA-Dependent  
1189 Protein Kinase PKR Is Required for Activation of NF- $\kappa$ B by IFN- $\gamma$  in a STAT1-  
1190 Independent Pathway. *J Immunol* 2001. doi:10.4049/jimmunol.166.10.6170.
- 1191
- 1192



